Intraneuronal Tau Misfolding Induced by Extracellular Amyloid-β Oligomers

Lauren Kathleen Rudenko

Burke, VA

B.S., James Madison University, 2010

A Dissertation presented to the Graduate Faculty of the

University of Virginia in Candidacy for the Degree of Doctor

of Philosophy

Department of Biology

University of Virginia

August, 2019

Abstract

Abnormal folding and aggregation of the microtubule-associated protein, Tau, is a hallmark of several neurodegenerative disorders, including Alzheimer's disease (AD). Although normal Tau is an intrinsically disordered protein, it does exhibit tertiary structure whereby the N and C-termini are often in close proximity to each other and to the contiguous microtubule binding repeat domains that extend C-terminally from the middle of the protein. Unfolding of this paperclip-like conformation might precede formation of toxic Tau oligomers and filaments, like those found in AD brain. While there are many ways to monitor Tau aggregation, methods to monitor changes in Tau folding are not well established. Using full length human 2N4R Tau doubly labeled with the Förster resonance energy transfer (FRET) compatible fluorescent proteins, Venus and Teal, on the N- and C-termini, respectively (Venus-Tau-Teal), intensity and lifetime FRET measurements were able to distinguish folded from unfolded Tau in living cells independently of Tau-Tau intermolecular interactions. When expression was restricted to low levels in which Tau-Tau aggregation was minimized, Venus-Tau-Teal was sensitive to microtubule binding, phosphorylation and pathogenic oligomers. Of particular interest is our finding that amyloid-β oligomers (AβOs) trigger Venus-Tau-Teal unfolding in cultured mouse neurons. We thus provide direct experimental evidence that AβOs convert normally folded Tau into a conformation thought to predominate in toxic Tau aggregates. This finding provides further evidence for a mechanistic connection between Aβ and Tau at seminal stages of AD pathogenesis.

Acknowledgements

This work was completed as part of the requirements for a Ph.D. degree for LKR. The authors would like to thank LKR's dissertation committee (Drs. Chris Deppmann, Sarah Siegrist, Bettina Winckler and Adrian Halme), Drs. John Lazo, Beth Sharlow and Murat Koseoglu, and the following past and current members of the Bloom lab (Drs. Erin Kodis, Shahzad Khan, Dora Bigler-Wang, Eric Swanson, Antonia Silva, and AndreÅLs Norambuena, and Nutan Shivange, Merci Best and Victoria Sun) for their intellectual input throughout the course of this study. This work was supported by NIH/NIA grant RF1 AG051085 (GSB), the Owens Family Foundation (GSB), NIH/NIGMS training grant T32 GM008136, which provided 2 years of support for LRK, Alzheimer's Association Zenith Fellowship ZEN-16-363266 (GSB), the Cure Alzheimer's Fund (GSB, John Lazo and Beth Sharlow), and NIH/Office of the Director Funds award OD016446 to purchase the Zeiss 780 microscope that was used throughout these studies (AP).

Table of Contents

Abbreviations

AA - arachidonic acid

Aβ – Amyloid-beta

AβOs - Amyloid-beta oligomers

AD – Alzheimer’s Disease

APP – Amyloid precursor protein

B4M - benzophenone-4-maleimide

CCR – Cell Cycle Re-entry

CFP - cyan fluorescent protein

CNS – Central nervous system

DMEM - Dulbeco's Modified Eagle's Medium

DTT – dithiothreitol

E% - Efficiency of energy transfer

FBS – Fetal Bovine Serum

FRET - Förster resonance energy transfer

FLIM – fluorescence lifetime imaging microscopy

FTD – Fronto-temporal Dementia

FTDP-17 - Frontotemporal dementia and parkinsonism linked to chromosome 17

HFIP - 1,1,1,3,3,3-hexafluoro-2-propanol

MAP – Microtubule-associated protein

MCI – Mild Cognitive Impairment

MT – Microtubule

MTBR – Microtubule binding repeat

mTFP – monomeric teal fluorescent protein

NMDA - N-methyl-D-aspartate

OA – Okadaic Acid

PrP – prion protein

ROI – Region of Interest

SplitFP - split fluorescent protein

TauT – Tau-teal

TauV – Tau-venus

TCEP - Tris(2-carboxyethyl)phosphine

Ttau – Teal-tau

TtauV – Teal-tau-venus

Tm - Lifetime

Vtau – Venus-tau

VtauT – Venus-tau-teal

WT – Wild-type

YFP - yellow fluorescent protein

Chapter 1: Introduction

Chapter 1: Introduction

Alzheimer's Disease: Historical Context of Dementia

The gradual loss of cognitive ability has long been associated with aging, but ancient writings reflected a lack of scientific understanding about distinctions between normal aging and pathology. Early attempts to explain loss of cognition gained some specificity with Plato and Aristotle in the fourth century BC. Plato describes the "bitter and bilious" humors which, when trapped inside the body, wreak havoc. Everything from forgetfulness and stupidity to rashness or cowardice were attributed to the balance of these humors. Aristotle blamed the maladies of old age on the cold black bile of the body [1]. In fact, old age itself is often discussed as an illness, during writings of this time period, but one that is inevitable.

One of the first to indicate that the cognitive decline of old age need not be inevitable came from the Roman philosopher, Cicero, who claimed that mental failure was in fact, the result of a weakness of will. Cicero considered it the moral duty of humanity to fight senility, and the means of doing so is by the exercise of physical and mental activity [2] ,a concept which has validity even today. With the writings around 100 BCE of Posidonius, a Greek philosopher, there began to develop an understanding and a terminology to differentiate normal mental decline from the loss associated with pathology or madness. This difference was expressed as the concepts of morosis and delirium. Delirium was a condition of the old, an expected loss of mental faculty over time. Morosis, on the other hand,

also appears in the young and is specifically associated with illness or madness [1]. The seeds of this differentiation were planted, but would not germinate until much later. In the 16th century attempts were made to categorize different types of mental illness, distinguishing conditions such as fever-induced delirium, madness and lethargy, from memory loss or the loss of reason. Finally, in the 1600's Thomas Willis wrote that morosis is "not improperly reckoned among the diseases of the head or brain" and suggested many potential reasons for this degeneration. [2] It was not until the 1860's that, thanks to a growing acceptance of the autopsy, the loss of brain mass accompanying aging and insanity was noted. In 1864, a physician named Samuel Wilks definitively described the cerebral atrophy that we now know is due to neuron loss. [3].

Historical context of Alzheimer's Disease

The first identification of a histopathology which would come to characterize Alzheimer's disease, the accumulation of plaques in an epileptic patient, was actually discovered by Blocq and Marinesco in 1892 and then by Redlich in two cases of senile dementia. In 1903 an improved silver staining method was developed by Bielschowsky which made neurons visible. This stain was used by Alois Alzheimer a few years later on the case that would identify the form of dementia which would carry his name [2]. In 1906, Alois Alzheimer gave the first description of the behavior and pathology of a patient, Auguste Deter, who died of an unknown form of dementia. Her behavior was described as

“delusional, forgetful, disoriented, anxious, suspicious, unruly and disruptive” and had declined rapidly over the past year [4]. After her death, Alzheimer used the newly improved method of silver staining to visualize and describe foci within the cortex and fibers inside otherwise normal appearing cells. These structures would become known as the pathological hallmarks of the disease, extracelluar plaques of Aβ (amyloid-beta) peptides and intraneuronal neurofibrillary tangles of the microtubule associated protein, tau.

Alzheimer’s disease (AD) is now known to be the most common form of dementia [5], impacting nearly 6 million patients in the United States alone [6] with the number projected to rise more than 2-fold by the middle of the century if efforts to prevent or slow disease onset fail. It is the sixth leading cause of death in the United States (and the fifth among the population above the age of 65. The cost of care for these patients is estimated exceed 270 billion dollars in 2019 [6]

The neurodegenerative effects of AD contribute to progressively worsening behavioral symptoms. Most patients with Alzheimer’s disease experience a slow development of symptoms over several years. Loss of neurons in the hippocampus, which plays a role in the consolidation of short-term memory into long-term memory as well as spatial orientation, results in short-term memory deficits and spatial disorientation that worsens as damage to the brain becomes more severe. Among the behavioral hallmarks of AD are confusion of time and date, wandering, and language impairment[7].

Due to its neurodegenerative nature, the severity and rate of degeneration varies among patients but progress through several stages. The initial

presymptomatic stage of the disease can last for decades and is a complicating feature of the disease, and combined with a lack of prophylactic treatments, makes early treatment impossible. When the first behaviorally identifiable symptoms develop it is referred to as mild cognitive impairment (MCI.) Patients in this category will begin to have difficulty with routine tasks and become disoriented intermittently. Symptoms eventually develop into the more severe "dementia due to Alzheimer's." [8] Patients with severe AD are incapable of living independently due to inability to complete the most basic of self-care tasks and an increasing toll on their physical health, including the ability to eat, drink and swallow.

Until recently, a definitive diagnosis of AD requires a post-mortem brain autopsy. However, there are diagnostic criteria in place for determining whether a living patient has possible or probable AD [9,10]. These involve a combination of psychiatric tests, PET imaging for plaques, biomarker analysis of cerebrospinal fluid, and various exclusionary tests to rule out non-AD dementias [6]. While there are no current disease-modifying drugs for AD, there are two types of FDA approved treatments which target synaptic transmission in an attempt to slow the behavioral effects of the disease. Four approved drugs are cholinesterase inhibitors which prevent the breakdown of the neurotransmitter acetylcholine in the brain. This is meant to combat the low levels of acetylcholine in the brains of AD patients [11-14]. The other is an NMDA receptor antagonist which targets neuronal excitotoxicity by preventing excess calcium entry into neurons [15].

Aβ and APP processing

Aβ is one of the two hallmark proteinaceous markers of AD, known for forming the extracellular plaques that characterize the later stages of the disease. Aβ comprises species of varying length from ~36 to ~43 amino acids long, but all contain the same core structure [16]. This peptide is formed by the cleavage of the amyloid precursor protein (APP) which can be cut by various secretases in one of two pathways that result in the production of non-amyloidogenic APP fragments either with or without Aβ. Three cleavage sites are particularly important for APP processing and Aβ production. The α-secretase site is cleaved by enzymes from the ADAM (a disintegrin and metalloprotease domain) family; the β-secretase site is cut primarily by beta-site APP cleaving enzyme BACE1, and the γ-secretase site is cleaved by a γ-secretase enzyme complex including presenilin (PSEN) [16-19] When APP is processed via the non-amyloidogenic pathway a sequential cut by α-secretase followed by γ-secretase results in three peptides; an N-terminal sAPPα, the APP intracellular domain and p3. Because the α-secretase cleavage site at Lys686 is within the potential Aβ sequence, this pathway prevents the production of Aβ entirely. Alternatively, APP can be processed by the amyloidogenic pathway. When this occurs, APP is cleaved by β-secretase and γ-secretase sequentially and an Aβ peptide is formed. Variation in α-secretase: β-secretase cleavage ratio would, therefore, shift the population of downstream peptides formed by APP processing to produce more or less Aβ peptide.

Familial mutations that effect this pathway are named for the locations of families first known to possess them. The Flemish and Swedish mutations, for

example, contain mutations near the α-secretase and β-secretase cleavage sites of APP respectively. Both favor cleavage by the Aβ producing β-secretase pathway, by respectively decreasing the affinity of α-secretase for its site or increasing the affinity of β-secretase for its site [20]. The processing of APP can also be shifted in the opposite direction. A673T, also known as the Icelandic mutation, is adjacent to the β-secretase site in APP, and results in a 40% reduction in processing of APP via amyloidogenic pathway. [21].

The study of Down's syndrome patients with an extra copy of the *APP* gene, provides additional evidence that APP processing is crucial to AD. These patients have elevated levels of Aβ and AD-like pathology, but not when the APP-containing portion of the third chromosome 21 is missing [22-24]. These genetic factors demonstrate a link among APP processing, Aβ accumulation and risk of disease development. In view of this evidence, a predominant theory of AD development, the "amyloid cascade hypothesis," proposes that it is the accumulation of the Aβ peptide that instigates the other pathological effects [25-27].

Risk Factors

AD is broadly divided into two categories. Early-onset AD is so named for the development of symptoms prior to the age of 60 – 65 years and makes up an estimated 1-6% of cases. Most cases of early onset AD come from families with a known history of AD, with about 13% inherited from autosomal dominant mutations with multiple generations effected [28]. Early-onset familial AD (FAD)

has a very strong genetic component and is characterized by an aggressive early-onset presentation of the disease in patients between 30-60 years of age, with most patients not living beyond 50 [29,30] Mutations that cause FAD occur in only 3 genes, the APP gene, PSEN1 and PSEN2. These mutations are fully penetrant and involve alterations in the processing of the trans-membrane amyloid precursor protein (APP) leading either to overall increase in Aβ levels or an increase in aggregation-prone forms of Aβ [31,32].

The majority of cases of AD are characterized as sporadic, though these too can be either early or late onset. Late-onset Alzheimer's disease is characterized by the development of symptoms after the age of 65. These cases have a more nebulous cause, with a broad spectrum of genetic risk factors and environmental factors.

By far, the greatest risk factor for developing sporadic AD is age and 81% of patients with AD are over 75 years old [33]. The close tie of AD with age also means that despite the already staggering numbers, AD is prone to underreporting, with some cognitive degeneration attributed inappropriately to simple age-based decline. Other risk factors include a family history of AD. Even among the sporadic cases of AD, having a relative with the disease doubles the risk of developing the disease [28]. While there does not always seem to be a single genetic component to this risk, it may be due to a combination of genetic risk factors not thoroughly defined, or the shared environment of families or some combination of the two. Genome-wide association studies have been done to try to pinpoint some of the genes that may contribute at lower penetrance levels [34-

36].

The strongest genetic component of AD, and one that is closely tied to onset of AD earlier than age 65, is the *APOE4* allele. The ApoE protein forms lipoproteins, binding with cholesterols, fats and peptides for transport through the blood stream, and its gene is present in humans as 3 common alleles: *APOE2*, *APOE3* and *APOE4*. A carrier of the *APOE4* allele is not guaranteed to develop AD, but a single copy increases risk 3-5-fold and 2 copies increase the risk up to 10-fold or more [6,37-39]. There is evidence that the *APOE4* allele contributes to pathology via stimulating oligomerization of Aβ as well as inefficient clearance of Aβ compared to E2 or E3 alleles [38,40-43] One allele of *APOE* actually appears to have a protective effect. This protective allele, *APOE2* has also been implicated in a signaling cascade which can affect other pathological hallmarks of AD including tau hyperphosphorylation [44] and phosphorylation of the NMDA receptor, contributing to synapse function, learning and memory.

Numerous studies and corresponding meta-analyses have also shown traumatic brain injury (TBI) to be a risk factor for sporadic AD, with increases in Aβ levels and plaques a well-documented result of these injuries [45-49]. Other risk factors include elements associated with cardiovascular health, leading to the general idea that what is good for the heart is good for the brain. Smoking, and second-hand smoke, obesity, diabetes, high cholesterol and hypertension are all associated with modest increased risk of dementia later in life [50-53].

The Aβ / tau connection

Until recently, the accumulated Aβ plaques themselves were thought to cause damage in AD. However, there is a weak correlation between dementia severity and plaque load in AD mouse models or humans [54,55]. In fact, immunizing with full length $A\beta_{1-42}$ is able to reduce plaque burden without preventing cognitive decline in humans [56,57]. These indications of the limited toxicity of fibrils and plaques are sometimes utilized as evidence against the amyloid cascade hypothesis, indicating that amyloid is not playing as significant of a role in AD as might be indicated by the genetic evidence. But the relative biological inactivity of fibrils and plaque deposits could also suggest that a different species of Aβ is neurotoxic. More recent attempts to correlate Aβ with behavioral and cognitive deficits have focused on soluble Aβ instead of plaque counts. Aβ peptides in different oligomerization states can have vastly different cellular effects. Monomeric Aβ has long been known not to have cytotoxic effects but oligomers ca be more synaptotoxic or cytotoxic [58,59]. When examined in this way, there does appear to be a good correlation of Aβ oligomers (but not plaques) with cognitive deficits [60,61]. Aβ oligomers in the absence of fibrils have been shown to have toxic effects in cell based assays and Aβ immunization of AD model mice can result in behavioral recovery without lowering plaque burden, suggesting an effect on a soluble Aβ pool rather than plaque deposits [56,62,63].

While amyloid accumulation in brain appears to be necessary for AD development, it is not sufficient and many, if not most, toxic effects of Aβ

oligomers depend on the presence of tau. This led to much disagreement in the field about whether to consider Aβ or tau the primary disease causing protein in AD [64]. In 2001, however, a pair of papers was published showing the link between the two pathologically aggregated proteins in AD. These papers demonstrated that in a mouse model overexpressing mutant tau, tau pathology could be worsened by the injection of Aβ [65] or by crossing with a mouse overexpressing mutant APP [66]. Additionally the deficits in mice overexpressing mutant human APP could be ameliorated by crossing mice into a tau null background [67]. Since then there has developed an extensive literature emphasizing how Aβ signals through tau to cause synapse damage [68], microtubule disassembly [69], NMDA excitotoxicity [70], trafficking deficits [71,72], ectopic neuronal cell cycle re-entry [73], cytotoxicity [74] and the mislocalization of tau into the somatodendritic compartment [72].

Given that several aspects of Aβ toxicity have been shown to be dependent on tau, indicating a functional link between these factors, deciphering the connection between these two hallmark proteins in the disease could be instrumental for the development of improved diagnostic criteria and treatments for AD.

Tau Structure and Function

Tau is a microtubule associated protein (MAP) which contains several important structural domains that mediate its physiological roles, folding and oligomerization. It has 0, 1 or 2 inserts of 29 amino acids each near its N-

terminus, a proline-rich region with many potential phosphorylation sites located near the end of the N-terminal half of the protein, and 3 or 4 imperfect, tandem microtubule-binding repeat domains (MTBRs) of 31 or 32 amino acids each located in the C-terminal half [75-77] Alternative splicing of exon 2, 3 and 10 create six splice variants of tau which differ by the number N terminal inserts and microtubule binding repeats [78].

The most well characterized physiological role for tau is its role in microtubule assembly and stabilization. Its discovery as a microtubule associated protein was, in fact, due to that role. In 1975 it was discovered that not only does tau co-purify with tubulin, upon separation from MAPs tubulin lost the ability to polymerize. The re-addition of tau to purified tubulin rescued the ability of tubulin to polymerize [79].

The function of the N terminal inserts is less well established though the varying length has some effects on spacing between microtubules [80] subcellular distribution and tendencies for aggregation [81]. The microtubule binding repeat region mediates the interaction of tau with microtubules with 4R isoforms having a higher affinity interaction than 3R isoforms and likewise promoting microtubule assembly more efficiently [75]. The second and third MTBRs are also responsible for Tau-Tau interactions in Tau aggregates [78].

Tau also has a role in the regulation of axonal transport. Axonal transport is driven by microtubule motors which carry materials along a network of microtubules. This network allows transport of cargo from the minus ends which cluster near the soma, to positive ends at a synapse that may be upwards of a

meter away [82]. Traffic moving towards the positive end (towards the synapse) is driven by a family of proteins called kinesins while transport towards the soma is driven by dyneins [82]. When overexpressed, tau inhibits the trafficking of vesicles, mitochondria and ER [83]. This inhibition of kinesin driven transport results in the buildup of cargo near the soma. The mechanism for this role of tau was elucidated by an experiment showing that fluorescently tagged kinesin motors when moving along a microtubule, have a tendency for pausing or detatching when they come into contact with a tau 'speedbump' while dyneins tend to reverse directions [84]. This, combined with a gradient of tau expression along an axon provides a potential mechanism by which cargo can be delivered to various places along an axon, rather than only be deliverable at the soma or synapse [85].

Though tau's primary expression is in the axon there is some localization of tau within the dendrite or nucleus. Tau also appears to have a role in the dendrite via targeting of the Fyn kinase to the dendrite which in turn regulates NMDA activity [70]. The loss of tau disrupts Fyn targeting to the post synapse and mitigates Aβ induced excitotoxity. There is some evidence that tau may have a role in stabilizing DNA and RNA as under conditions of heat stress, dephosphorylated tau accumulates in the nucleus and protects DNA from heat shock damage, [86] but this role is not as well characterized as axonal tau.

There are two general categories of mutations of tau which can affect these physiological roles. Missense mutations generally cluster near the MTBR. Some of these mutations include G272V, N279K, ΔK280, P301L, V337M or

R406W. These kinds of mutations usually have a decreased affinity for microtubules and are more prone to aggregation than wild type tau [87-89]. Splicing mutations on the other hand are often located near intron 10 and shift the 3R to 4R ratio, usually though not always increasing the amount of 4R compared to 3R [87].

Post-translational modifications of tau

Tau can be modified in many ways including phosphorylation, acetylation, methylation, glycation, isomerization, *O*-GlcNAcylation, nitration, sumoylation, ubiquitination, and truncation. Some of these modifications are more well studied than others, and none so much as the role of phosphorylation on tau both in terms of function and pathology. There are over 80 potential phosphorylation sites on the longest form of tau and over half of them have been observed in vivo [87]. When brains of normal adults are compared to AD post autopsy, AD brain carries approximately four times the number of phosphorylations [90]. Some of these phosphorylation sites are inside or flanking the MTBR and modulate tau's binding to microtubules. S262, among others, has been shown to lower the affinity of tau for microtubules [91]. Other pathological processes have different subsets of necessary phosphorylation sites. For example, the Aβ induced ectopic cell cycle re-entry (CCR) characterized in our lab and others requires phosphorylation of Tau at Tyr18, Ser409 and Ser416 [73].

Not only can phosphorylation directly affect the ability of tau to bind microtubules, phosphorylated tau can sequester normal tau and other

microtubule associated proteins preventing ‘normal tau’ from functioning, thus disrupting microtubule assembly. Reversing this phosphorylation load of AD tau using protein phosphatases rescues tau’s ability to support microtubule assembly *in vitro* and diminishes tau pathology *in vivo* [92].

The phosphorylation of tau is regulated by a balance of many kinases and phosphatases. Phosphorylation of the sites required for CCR is driven by Fyn, CaMKII and PKA [73]. Other kinases include glycogen synthase kinase 3β (GSK3β), cyclin-dependent kinase 5 (CDK5), mitogen-activated protein kinase (MAPK) and JUN n-terminal kinase and microtubule affinity-regulating kinase (MARK)[87].

Hyperphosphorylation can also be driven by the reduction in phosphatase activity of which several have been implicated in tau dephosphorylation. PP2A accounts for approximately 70% of overall phosphatase activity of tau [93] and in AD brain has a reduced activity of between 20 and 40%. The remaining 30% of tau dephosphorylation is regulated by a combination of phosphatases PP1, PP2B, PP2C and PP5. Okadaic acid, a phosphatase inhibitor utilized experimentally in this work, was selected for its effects on this system, targeting primarily PP1 and PP2A [94] to increase phosphorylation of tau.

Prion-Like pathology

Recent work has shown that some aspects of AD pathogenesis have elements in common with prion diseases. Prion diseases were first described in Creutzfeldt-Jacob disease where it was determined that prion protein pathology spreads cell

to cell without the need for a DNA or RNA based intermediate. [95,96]. Other prion-based diseases, such as mad cow disease, scrapie and kuru do differ from AD in that there is no evidence for AD being spread from person to person the way true prion diseases spread. Even so, there is some evidence for prion-*like* pathology. The hypothesis that AD may have prion-like characteristics comes from the fact that AD pathology seems to spread along synaptically connected pathways, with a temporally defined spread beginning in subcortical regions, the transentorhinal cortex and entorhinal cortex (Braak stages I and II.) Pathology then spreads to the hippocampal formation and some parts of the neocortex (Braak stages III and IV), followed by most of the neocortex (Braak stages V and VI.) [97,98]

Early *in vivo* work showed that tau expressing mice without tau pathology could be induced to form intracellular inclusions by the injection of exogenous tau inclusions. The pathology that develops spreads from the injection site to distant brain regions [99]. Additional *in vivo* evidence for the cell-to-cell spread of tau pathology comes from mouse lines expressing mutant tau in the entorhinal cortex. These two mouse models develop pathology outside the entorhinal cortex made up of endogenous mouse tau, indicating an *in vivo* cell to cell transmission of misfolded tau. [100,101]

In vitro, a series of experiments used a combination of MTBR aggregates and YFP labeled full length tau to show that MTBR aggregates could be taken up by non-neuronal cells and induce the aggregation of endogenous full length tau. Furthermore, the induced aggregates were themselves able to serve as a

template to induce aggregation of tau monomer and transfer between co-cultured non-neuronal cells [102].

Tau folding and conformation

Monomeric Tau is a natively unfolded protein. *In vitro*, it behaves predominantly like a random coil and small-angle X-ray scattering and NMR do not show a stable secondary structure [103]. It is highly hydrophillic and soluble [104], heat stable and does not spontaneously form filaments [103,105,106]. To aggregate in vitro, tau requires the presence of a strong anion like heparin or arachadonic acid (AA) [107,108]. Despite its low tendency to aggregation, paired helical filaments [109] and neurofibrillary tangles (NT) are hallmarks of many neurodegenerative diseases, including AD. The abnormal tau aggregation into the straight and paired helical filaments characteristic of tauopathies is driven by a shift from random coil to a β-sheet structure of regions within the second and third repeat domains [110]. This shift to β sheet structure can be seen by circular dichroism spectroscopy, Fourier transform infrared spectroscopy and X-ray diffraction and requires a set of two hexapeptides located in the second and the third repeat of the tau MTBR [78,110,111].

There is evidence that Tau assembly into filaments depends on an interaction between its terminal ends and the MTBR. While the interaction of the C-terminus promotes solubility [112] the interaction of the N-terminus promotes aggregation. This form of Tau is recognized by two conformation-dependent antibodies, Alz50 and MC-1, which label Tau in early AD brain [113,114]. Both

antibodies recognize similar, but distinct discontinuous epitopes formed by short stretches of amino acids near the N terminal and a region in the MTBR.

In 2006, two papers utilized two separate experimental techniques independently to approach the issue of tau conformation in solution, both coming up with a similar folded configuration that would become known as the paperclip or hairpin model. This model indicates that the N- and C- termini are close together with the C-terminal held closer to the MTBR [115,116] In the first of these papers, FRET pairs were created along the distance of 2N4R, 2N3R or 0N3R tau protein by the insertion of tryptophans (of which there are none intrinsically.) This was paired with a labeled cysteine acceptor inserted by mutation or from one of two intrinsic cysteine with input from other cysteines muted by mutation to alanine. Exchanges and insertions were as conservative as possible by mutating a hydrophobic amino acid into the necessary tryptophan and a polar amino acid into cysteine [116].

While it is possible that these mutations could change the structure of tau *in vitro*, the group did confirm via circular dichroism microscopy that the spectra were largely unchanged by these mutations. Additionally, both unmutated and mutated tau was able to stimulate tubulin assembly *in vitro*. Using these constructs and calculated FRET distances they determined that while tau shows great flexibility and mobility *in vitro,* there is some secondary structure. Their calculations indicated a model in which the C-terminus is held within FRET distance of the R2/R3 repeats and the N-terminus is held close to the C-terminus but outside of FRET distance of the repeat domain. These calculated distances

combined serve as the basis for the ‘hairpin’ model of tau folding.

The second group further sought to characterize this conformation and its role in the transition between loosely structured monomer to tightly ordered filament, by focusing on the effect of the N-terminus on tendency to aggregate [115]. Using a truncated version of tau containing the N-terminal portion of the alz-50 epitope, they demonstrated that expression of an excess of this fragment inhibits the polymerization of full-length tau protein, in a manner that requires the presence of certain portions of the C-terminus. Taken together with what is known from conformation specific antibodies like alz-50, their work supports the model of tau folding in which the N-terminus interacts with the C-terminus to stabilize the protein in its soluble form. Additionally, this supports a model in which the loss of C-terminus association with the MTBR (and subsequent interaction of the N-terminus with that region as in conformation sensitive epitopes) could be a key to the conversion of normal Tau into a toxic, misfolded form.

Biomarkers and biosensor development

Current biomarkers largely depend on the identification of amyloid or tau at later stages of pathology. Among these include a well-documented decrease in cerebral spinal fluid (CSF) levels of $A\beta_{1\text{-}42}$ as Aβ is sequestered into plaques, which is not reliably mirrored in blood plasma. [117] Plaque burden can also be visualized via the now widely accepted compound known as Pittsburgh Compound-B [118] for PET imaging.

Biomarkers for tau pathology have also been widely researched. PET imaging for tau aggregation [119] as well as monitoring of total and phosphorylated tau in CSF [120] are among the researcher's arsenal for determining the extent of tau pathology in the brain. Results from blood plasma are more mixed, with phosphorylated tau not reliably measured and total tau measurable but correlating weakly with large overlaps between normal aging and pathological samples [121] but sensitivity has improved making plasma biomarkers an improving possible diagnostic tool. [117,120]. The role of a biosensor differs from that of a biomarker as it would allow the probing of a sample or treatment for an effect on tau folding specifically, either in live cells in the context of a laboratory tool, as it is used in this work, or as a potential diagnostic tool.

Several approaches were considered for the development of this biosensor and both splitFP and FRET constructs were developed. The splitFP constructs were considered for their smaller tag, the possibility of a binary on/off signal and ease of analysis but when tested did not prove usable for reasons that will be discussed in chapter 5. The next stage was the development of a Förster resonance energy transfer (FRET) biosensor which would serve as the same kind of readout.

FRET serves as a quantitative measure of dynamic protein-protein interactions. In order to develop an intramolecular biosensor, instead of labeling two different proteins, a donor and an acceptor fluorophore are added to the N and C-terminus to allow quantitation of the distance between the two. There are

many possible FRET pairs that can be used, among the most common are versions of fluorescent protein (CFP) and yellow fluorescent protein (YFP). In development of this biosensor mTFP (monomeric TFP) was used as a donor. TFP is monomeric, quicker maturing, brighter, more pH stable and with a higher quantum yield than CFP[122,123]. Likewise the YFP variant Venus was selected for its optical characteristics, including a more rapid maturation time and decreased sensitivity to environment compared to previously common acceptor fluorophores [124].

FRET involves transfer of energy from the donor to the acceptor and when a donor acceptor pair are within FRET compatible distance, the donor is quenched and the acceptor is sensitized. This results in a dimmer donor signal and brighter acceptor signal in FRETing situations. Intensity (confocal) FRET is a form of FRET microscopy which quantifies this transfer of energy by measuring the intensity of multiple channels of excitation and emission, using background subtraction and single labels to calculate an efficiency of energy transfer (E%) for a given pixel or ROI. Fluorescence lifetime imaging microscopy (FLIM) also calculates an E% but does so by instead measuring the average time a molecule stays in an excited state before emitting a photon and returning to ground state. Each fluorophore has an intrinsic lifetime that is unique to itself, and changes if energy is transferred to an acceptor [125]. FLIM lifetime is very sensitive to microenvironment but insensitive to fluorophore concentration or excitation intensity. Additionally, no background subtraction of contaminating signal is required, as only the donor lifetime is being measured. It also provides more

information in the calculated result, taking into account the percentage of donor that is quenched and unquenched in a sample [126]. For this reason, FLIM was used as a readout whenever intensity sensitivity was not required by the experimental design.

Summary:

While a great deal is known about the pathology and spreading of tau in AD, there is still much to be learned about the early events that precede the spread of toxic pathology. Evidence in the literature is consistent with a folded structure of tau that, when unfolded, may serve as a pathological preamble to toxic oligomers and filaments. While there are many tools available to monitor filaments and aggregates of tau, as well as some to monitor oligomeric tau, this work fills a gap in building a tool to monitor a conformation change in tau that previously could only be seen in fixed samples with a small number of conformation dependent antibodies. The development of this biosensor is accompanied by experimental evidence that emphasizes the need to distinguish intermolecular from intramolecular signals, not only when analyzing this particular biosensor, but biosensors in general, an issue that has been largely ignored in the field of biosensors. Finally, this tool allowed the identification of a mechanistic link between amyloid-β oligomers (AβOs) and tau misfolding which strengthens the connection between Aβ pathology and Tau pathology at early stages of AD development.

Chapter 2: Materials and Methods

Chapter 2: Materials and Methods

Cell culture

Cell culture reagents were from Gibco/Invitrogen unless specified otherwise. Primary cortical neurons were isolated from wild type (C57/Bl6) mouse embryos aged approximately 18 days as previously described [72,73], except that phenol red-free Neurobasal medium was used exclusively. CV-1 African green monkey kidney cells (ATCC catalog # CCL-70) were maintained in Dulbeco's Modified Eagle's Medium (DMEM) with 10% fetal bovine serum and 50 µg/ml gentamycin, and were dissociated with TyrpLE Express (Thermo Fisher) for subculturing. For live imaging, CV-1 cells and neurons were plated onto 14 mm #1 glass-bottom MatTek dishes.

Fluorescent fusion proteins

Expression vectors for singly and doubly labeled Tau are in the background vector pCSC-SP-PW-NepX (pBOB-NEPX; from Inder Verma, Addgene plasmid # 12340). Human 2N4R Tau coding sequence was inserted between the Age1 and HpaI restriction sites by standard restriction digest techniques. The gene for the fluorescent proteins, mTFP (Teal) [122] and Venus [124]. were then inserted at the N-terminal Age1 site or the C-terminal HpaI site, and confirmed for sequence accuracy and direction of insertion. The expected spectral properties and sizes of all fluorescent fusion proteins were confirmed by spectral imaging and western blots using mouse monoclonal Tau5 antibody [127]. Constructs were then inserted into lentivirus with the packaging vectors

pMD2.G (from Didier Trono, Addgene plasmid # 12259) and psPAX2 (from Didier Trono, Addgene plasmid # 12260) using the lentiviral protocol provided by Thermo Fisher for Lipofectamine 3000 production of lentivirus (Thermo Fisher L3000015.)

Western Blotting

Western blots for the supplemental figure were run using Bio-Rad 10% mini-PROTEAN pre-cast gels in Tris/Glycine SDS running buffer. Boiled samples were run alongside precision Plus Protein ladder (1610374). Staining for tau utilized mouse monoclonal Tau5 antibody (1:4000) **[127]** and mouse monoclonal anti-GFP NeuroMab clone N86/38 (1:1000) with secondary licor antibodies IRDye 800CW Donkey anti-Mouse IgG (926-32212) and IRDye 680RD Donkey anti-Mouse IgG (926-68072) at 1:10000. Phosphorylation stains were done with tau p262 (Anaspec AS-54973) and P-threonine (Cell Signaling 9381). Tau oligomer antibodies TOC-1, TOMA-1 (Millipore). Tau oligomer antibodies TTC-35**[128]** and TTC-99 provided by Rakez Kayed.

Expression of fluorescent fusion proteins

Wild type neurons were transduced with lentivirus between day 8 and day 10 *in vitro*. CV-1 cells were infected at approximately 60% confluence to allow for easier imaging of individual cells. Expression was monitored until the fluorescence was visible on an EVOS FL microscope (ThermoFisher). Cells were

ready for imaging approximately 2 days post transduction for CV-1 cells and 4 days for neurons.

Imaging

For CV-1 cells, standard DMEM was replaced with phenol red-free DMEM prior to imaging. FRET imaging was done on the Zeiss 780 confocal/ NLO/FLIM microscope. Excitation for intensity FRET experiments used an Argon-ion laser (458 nm and 514 nm excitation; 455-500 nm and 526-579 emission). Confocal FRET images were acquired with GaAsP (Gallium Arsenide Phosphide) detector with approximately 40% quantum efficiency. 2-photon FLIM-FRET images were acquired by exciting the donor molecules with 820 nm excitation (em 480/40 nm) (Coherent Chameleon Vision-II Ti:Sapphire laser) . Becker & Hickl (Germany) Time correlated single photon counting (TCSPC) board (SPC-150) was used with a high-sensitivity hybrid GaAsP detector (HPM-100-40, 300-650 nm). Images were acquired with a 40X oil objective (1.30 NA). All live imaging was done on a temperature-controlled stage at 37º C with humidified 5% CO_2 gas flow to maintain pH and humidity.

Biological vs Technical replicates

Biological replicates are experiments repeated with different batches of cells, treatment reagents and imaging day.

Technical replicates were done with different batches of treatment reagents and sometimes different imaging day, but all use coverslips from a

single isolation of neurons or passage of CV1's. They untreated are generally more or less similar to each other depending on whether they were imaged during the same imaging session or on consecutive days.
There is obvious variation of the lifetime of the pre-treatment/control from imaging session to imaging session so all conditions are compared to a relevant control imaged in the same imaging session as they were.

Tau and Aβ oligomer preparation

Tau oligomers were prepared as described previously [72,129]. 2N4R Tau was brought to 4 μM in 100 mM Tris, 0.1 mM EDTA, 150 μM Tris(2-carboxy-ethyl)phosphine (TCEP; Life Technologies) and treated overnight with 50 μM benzophenone-4-maleimide (B4M; Sigma-Aldrich) then treated with 5 mM dithiothreitol (DTT; Roche) to inactivate B4M and dialyzed into 100 mM Tris, 0.1 mM EDTA and 5 mM DTT. A portion was removed and flash frozen for monomer treatments, and the remaining protein was aggregated overnight in the presence of 150 μM arachidonic acid (AA). The oligomers were treated for 5 minutes with UV light at 254 nm (Spectroline model EF-180), then flash frozen in small aliquots to be used immediately after thawing.

Amyloid-β oligomers (AβOs) were prepared from lyophilized synthetic Aβ(1–42) (AnaSpec), dissolved in HFIP (1,1,1,3,3,3-hexafluoro-2-propanol (Sigma- Aldrich Co.) to 1 mM and evaporated overnight at room temperature. The dried powder was resuspended in DMSO to 5 mM and sonicated for 10 minutes in a water bath. The peptide was then diluted to 100 *μ*M in Neurobasal

media, and incubated for 48 hrs at 4º C with rocking. Prior to use, oligomers were spun briefly to remove large oligomers and fibrils, bringing the concentration in solution to approximately 50 *μ*M.

Experimental Perturbation of Cells

Cells were imaged prior to any medium additions, and then nocodazole (Abcam) or okadaic acid (OA; Abcam) was added to a final concentration of 1 μM while the cultures remained in place on the microscope stage. One hour later the same fields of view were imaged again.

Aβ and Tau oligomer treatments were too long to be done on stage, so parallel coverslips were imaged for treated and control cultures for these conditions. For AβOs, neuron medium (Neurobasal + B27) was replaced with B27-free Neurobasal, and 1 hour later freshly prepared AβOs (see above) were added to the medium to a final concentration of approximately 1.5 μM total Aβ(1-42). Cells were imaged 6 hours later. For Tau oligomers, freshly thawed aliquots (see above) were diluted into medium to a final concentration of 250 nM total Tau 18 hours before imaging.

Thresholding for intramolecular FRET

Images were taken in parallel on the same system for intensity (confocal) FRET and 2-photon lifetime FRET (FLIM). It was determined that intensities below 750 – 1000 arbitrary units of acceptor intensity had minimal contamination of intermolecular FRET (see Figure 2.) Using the parallel images we determined

that this intensity range corresponded to a photon count of lower than approximately 500 on the 2-photon detector so cells were selected to be primarily within this expression range. All images then had single pixel regions of interest selected above background (varied slightly by experiment; usually 30-50 photons) and below a photon count of 500. Doing so excluded any cells or regions of cells that had a biosensor concentration that might have yielded significant intermolecular FRET.

FRET / FLIM analysis

FRET analysis was done largely in ImageJ (https://imagej.nih.gov/ij/) via a plugin written at the University of Virginia's Keck Center for Cellular imaging. This plugin allows subtraction of background and removal of spectral bleedthrough. After these corrections the result is a calculated E% (efficiency of energy transfer) for each ROI [130,131].

FLIM images were first analyzed by Becker & Hickl SPCImage software (https://www.becker-hickl.com/), Curve fitting procedures done as described previously[125,132]. Briefly, an exponential decay curve was fitted such that the Chi^2 was approximately 1 (with a two-component analysis of the donor, incomplete exponential decay and a measured instrument response function). These data were exported in a series of asc files. 2-photon images were used to designate single pixel regions of interest within the previously determined intensity range. A Fiji (https://fiji.sc/) macro written by Karsten Siller was then used to measure pixel intensity values in the selected ROIs and generate Excel

(Microsoft) based results files for each image, which included a calculated lifetime value for each pixel/papROI. Some additional manual filtering of the results to remove outliers was performed including any ROI's with a Chi^2 below .5 or above 2 (indicating the ROI was not well fitted by the decay curve). Lifetimes below 500 ps were also disregarded. These very low lifetimes were often seen outside of cells in the background, associated with very large Chi^2 values and were not in the reasonable range for the fluorophore (possibly due to any dying cells or degraded biosensors). Lifetimes were plotted as a frequency distribution histogram to determine the peak and distribution of the lifetime for each image/condition.

For each figure (3-6) a single "experiment" constitutes 6-9 fields of view per condition, with 1-2 cells per field of view. The number of ROI's analyzed per field of view/ experiment varied significantly based on how many were thresholded out (as background pixels, too bright, poor Chi^2, but most fields of view were in the range of 5-10 thousand analyzed ROI's after thresholding.

Statistical Analysis

GraphPad Prism 7 software was used to analyze each data set by t test, Kolmogorov-Smirnov test or one-way analysis of variance with a Tukey post-hoc test as appropriate.

Chapter 3: Characterization of a tau FRET biosensor sensitive to tau intramolecular folding

Chapter 3: Characterization of a tau FRET biosensor sensitive to tau intramolecular folding

To test whether Tau does, indeed, convert between folded and unfolded states in living cells, we developed and characterized a full-length Tau biosensor labeled at its N- and C-termini with FRET compatible fluorescent proteins.

Biosensor Development

Because Teal and Venus constitute an effective donor-acceptor pair for Förster resonance energy transfer (FRET), the N- and C- termini of full length tau were labeled with Venus and Teal fluorescent proteins respectively (Venus-Tau-Teal). Venus-Tau-Teal allowed us to visualize normally folded (paperclip/hairpin) and unfolded Tau in live cells that expressed the biosensor. Venus-Tau-Teal is operationally analogous to a previously described FRET biosensor from another group based on 0N4R Tau labeled with CFP and YFP [133]. A key distinction between the present study and its predecessor is that our approach ensured that intramolecular FRET signals, an indicator of the conformation of individual Tau molecules, was minimally contaminated by intermolecular FRET signals or FRET-inhibiting effects due to Tau-Tau aggregation.

By expressing Venus-Tau-Teal in CV-1 African green monkey kidney fibroblasts and primary mouse cortical neurons we obtained evidence that microtubule-associated Tau has a folded, paperclip/hairpin-like conformation that can be modulated by drugs affecting microtubule binding or Tau phosphorylation.

Most importantly, we found that amyloid-β oligomers (AβOs) cause Tau to unfold and adopt a conformation associated with toxic Tau aggregates. These observations provide direct evidence that AβOs control Tau conformation, and thereby constitute yet another example of how Aβ and Tau work together to drive AD pathogenesis [134].

To establish the optimal structure for a Tau folding biosensor, we designed Venus-Tau-Teal, Teal-Tau-Venus and four singly tagged fusion proteins: Venus-Tau, Teal-Tau, Tau-Venus and Tau-Teal (Fig. 1). The singly tagged proteins were necessary for calculating spectral bleed-through for intensity efficiency (E%) measurements [131] and the fluorescence lifetime of unquenched donor (Teal) for fluorescence lifetime imaging (FLIM) [123]. When expressed in CV-1 African green monkey kidney fibroblasts and imaged by confocal microscopy, all singly (Fig. 2) and doubly (Fig. 3) labeled fusion proteins localized to microtubules, indicating that coupling Teal, Venus or both to Tau does not obviously impair Tau's microtubule-binding activity.

Intermolecular vs Intramolecular FRET

Teal-Tau-Venus and Venus-Tau-Teal are capable, in principle, of producing intramolecular FRET. In addition, each protein is theoretically capable of aggregating to form oligomers or filaments resulting in intermolecular FRET. This potential signal from intermolecular FRET is generally overlooked in the field of biosensors but the data in this paper highlights that because of favorable orientations of Teal and Venus on adjacent fluorescent fusion proteins, or

causing attenuation of intramolecular FRET due to unfolding coupled with a parallel arrangement of individual fluorescent fusion proteins within aggregates.

To use a doubly tagged protein as a FRET biosensor for the folding state of Tau, we therefore had to identify conditions in which measured FRET signals are unaffected by fluorescent fusion protein aggregation. This was accomplished by analyzing Teal-Tau-Venus and Venus-Teal-Tau at various expression levels in CV-1 cells. More specifically, we sought to establish an expression range in which FRET efficiency (E%) is independent of expression level and signal is therefore is dominated by intramolecular FRET. Since an intermolecular FRET signal would be dependent on the amount of biosensor expressed, a significant effect of intensity on calculated E% would indicate the FRET signal is predominantly intramolecular within that range.

Expression levels were determined by measuring the fluorescence intensity of the acceptor fluorochrome, Venus, using the 514 nm argon laser line to excite Venus without exciting Teal. For each pixel of a measured intensity, an E% was calculated and the data was binned into expression levels as illustrated in figure 3. At low levels of biosensor expression, (bins up to 750-1000 arbitrary units of acceptor intensity), the increasing biosensor concentration did not have a significant effect on E%. At concentration ranges higher than this level, Venus-Tau-Teal yielded a concentration-dependent decrease in E%, indicating an intermolecular component to the signal.

In contrast, for Teal-Tau-Venus we did not observe a low Venus intensity range in which E% was independent of intensity. We therefore decided to use

Venus-Tau-Teal for all further experiments. Moreover, to minimize potential interference of intramolecular FRET caused by Venus-Tau-Teal aggregation, we restricted our data collection for subsequent experiments to cells and regions of interest (ROI's) in which the Venus intensity was less than this determined range of intensity.

Venus-Tau-Teal is sensitive to microtubule loss and protein phosphatase inhibition

To test whether Venus-Tau-Teal responds to cellular perturbations, we studied its properties under conditions in which microtubules or overall protein phosphorylation were manipulated. A 1 hour, 1 μM nocodazole treatment of CV-1 cells caused extensive microtubule depolymerization, a concomitant loss of Venus-Tau-Teal association with microtubules and a shift towards longer Teal fluorescence lifetime (Fig. 4A-D). This lifetime increase is indicative of decreased FRET efficiency, implying that Tau is predominantly in the paperclip/hairpin conformation when bound to microtubules and adopts a more open conformation when dissociated from microtubules. Treatment of CV-1 cells with the microtubule-stabilizing drug, taxol, which competes with tau for MT binding [135], was more inconsistent in its effects on Teal lifetime and those effects were of a smaller magnitude. (Discussed in chapter 4 supplement.)

Okadaic acid is a broad spectrum protein phosphatase inhibitor with a preference for protein phosphatase 2A which has been shown to cause several AD-like neuropathologies *in vitro* and *in vivo* [136]. Treatment of CV-1 cells for 1

hour with 1 μM okadaic acid caused an approximately 6-fold increase of phosphorylation at p262 (Sup. Fig 2) and a shortening of Teal fluorescence lifetime (Fig. 4.) While this decrease in Teal lifetime might be due to phosphate accumulation on tau, for which 85 phosphorylation sites have been identified (http://cnr.iop.kcl.ac.uk/hangerlab/tautable), increased phosphorylation of other proteins cannot be ignored as contributing factors.

Additionally, due to the established literature on phosphorylation-induced oligomerization of tau [137], the possibility that these effects are due to an intermolecular event such as oligomerization should not be ignored. While the method of analysis described excludes most intermolecular signal under basal conditions, oligomerization could cause intermolecular signal at lower concentrations. To further elucidate the differing lifetime shifts of nocodazole and okadaic acid, western blots of treated samples were probed for Alz50 reactivity (Sup. Fig.4) and several tau oligomer antibodies (TOC1, TOMA-1, TTC-35, TTC-99). Alz50 reactivity was increased in nocodazole treated cells compared to untreated and okadaic acid treated cells. As the C -terminus may move out of the way for the N-terminus to have access to the MTBR core in the Alz50 epitope [113,115], (thus decreasing FRET/ increasing lifetime), this is consistent with the lifetime data. The particular tau oligomer antibodies tested showed no increased reactivity over the control in either condition. As these tau oligomer antibodies are only reactive to particular oligomers, other untested tau oligomer antibodies may yet be able to pick up an oligomerization event that they did not. Regardless of what type of interaction is causing the decrease in lifetime, the response of

Venus-Tau-Teal to okadaic acid further indicates the responsiveness of this Tau folding biosensor to agents that affect cellular physiology.

Venus-Tau-Teal responds to pathological oligomers of Tau and Aβ

Extracellular Tau oligomers have been found to cause aggregation of intracellular Tau, accumulation of endogenous Tau in the somatodendritic compartment, alteration of fast axonal transport and synaptotoxicity [72,102,138]. Extracellular AβOs cause an additional set of adverse neuronal responses, such as impaired synaptic activity, ectopic neuronal cell cycle re-entry, which is a prelude to massive neuron death in AD [139], inhibition of nutrient-induced mitochondrial activity, and disruption of normal axon initial segment function [63,73,140-145]. Because the new results presented here so far indicate that Venus-Tau-Teal can serve as a biosensor for conversions between the compact, paperclip/hairpin and unfolded conformations of Tau, we next tested if extracellular oligomers of Tau or Aβ can alter Venus-Tau-Teal conformation.

After exposure of primary mouse cortical neurons to extracellular human 2N4R Tau oligomers for 18 hours, the Teal fluorescence lifetime of Venus-Tau-Teal shortened (Fig. 5). This decrease in lifetime, like that seen in okadaic acid treated cells, is consistent with prior evidence that extracellular aggregated Tau causes intracellular tau to aggregate [72,102]. In contrast, when primary mouse cortical neurons were exposed to AβOs for 6 hours, the Teal fluorescence lifetime of Venus-Tau-Teal increased (Fig. 6). This result indicates that AβOs induce Tau unfolding from the paperclip/hairpin conformation.

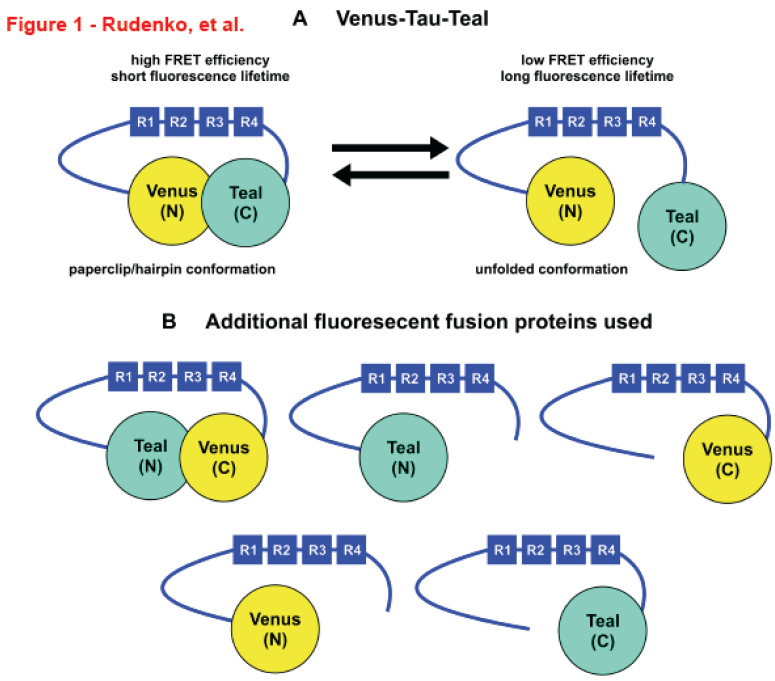

Fig. 1. Fluorescent Tau fusion proteins. Illustrated here are the fluorescent fusion proteins of human 2N4R Tau used in this study. A) Venus-Tau-Teal was compared with B) Teal-Tau-Venus for discriminating intramolecular from intermolecular FRET (see Fig. 3), and the singly labeled fluorescent fusion proteins in B) were used as standards for FRET efficiency (E%) and FLIM experiments. R1, R2, R3 and R4 signify the microtubule-binding repeat domains of Tau.

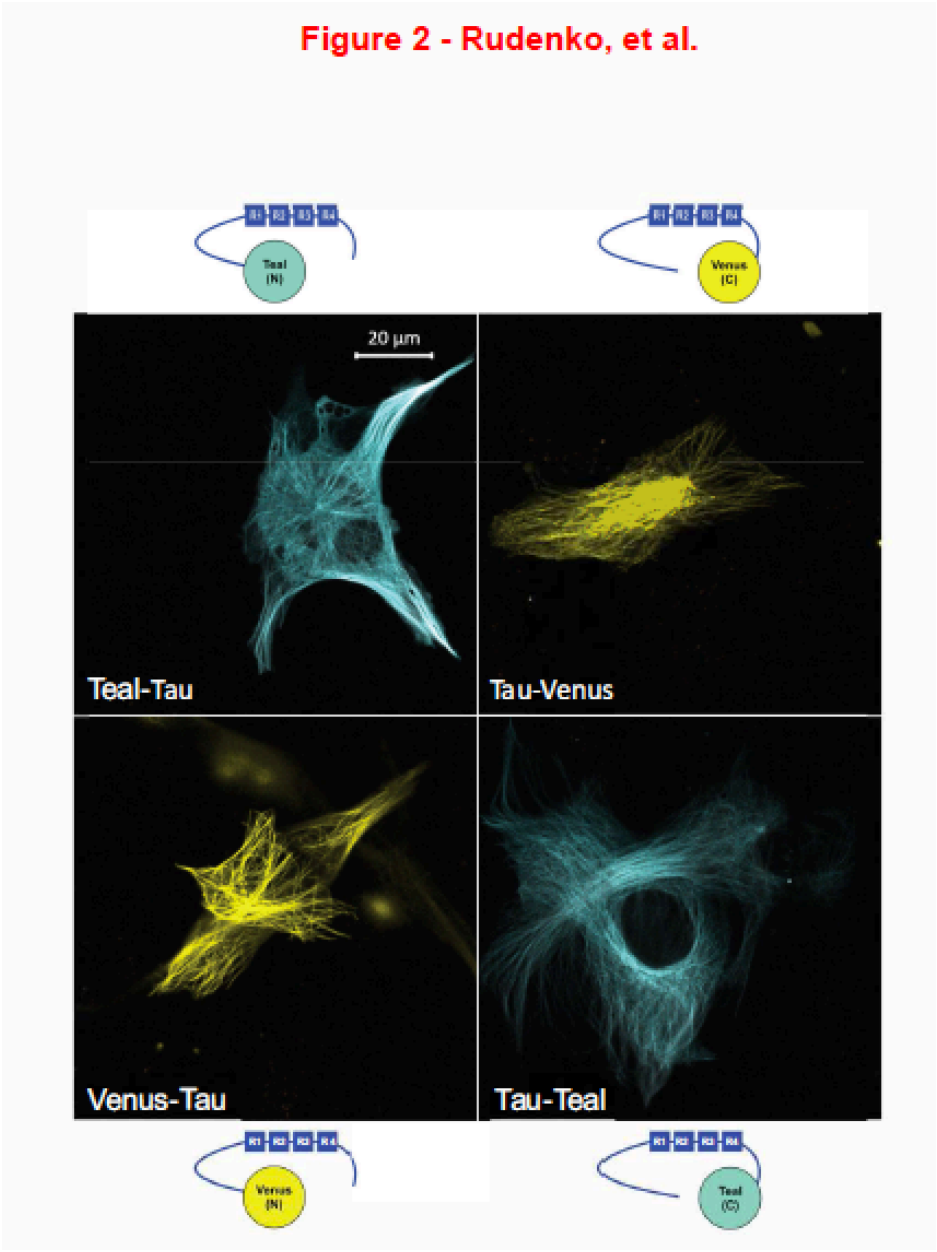

Fig. 2. Expression of singly labeled fluorescent Tau fusion proteins in CV-1 fibroblasts. All such fluorescent fusion proteins target to microtubules. These proteins were used for subtracting spectral bleedthrough for FRET efficiency (E%) measurements and for calculation of unquenched donor (Teal) fluorescence lifetime for FLIM experiments.

Figure 3 - Rudenko, et al.

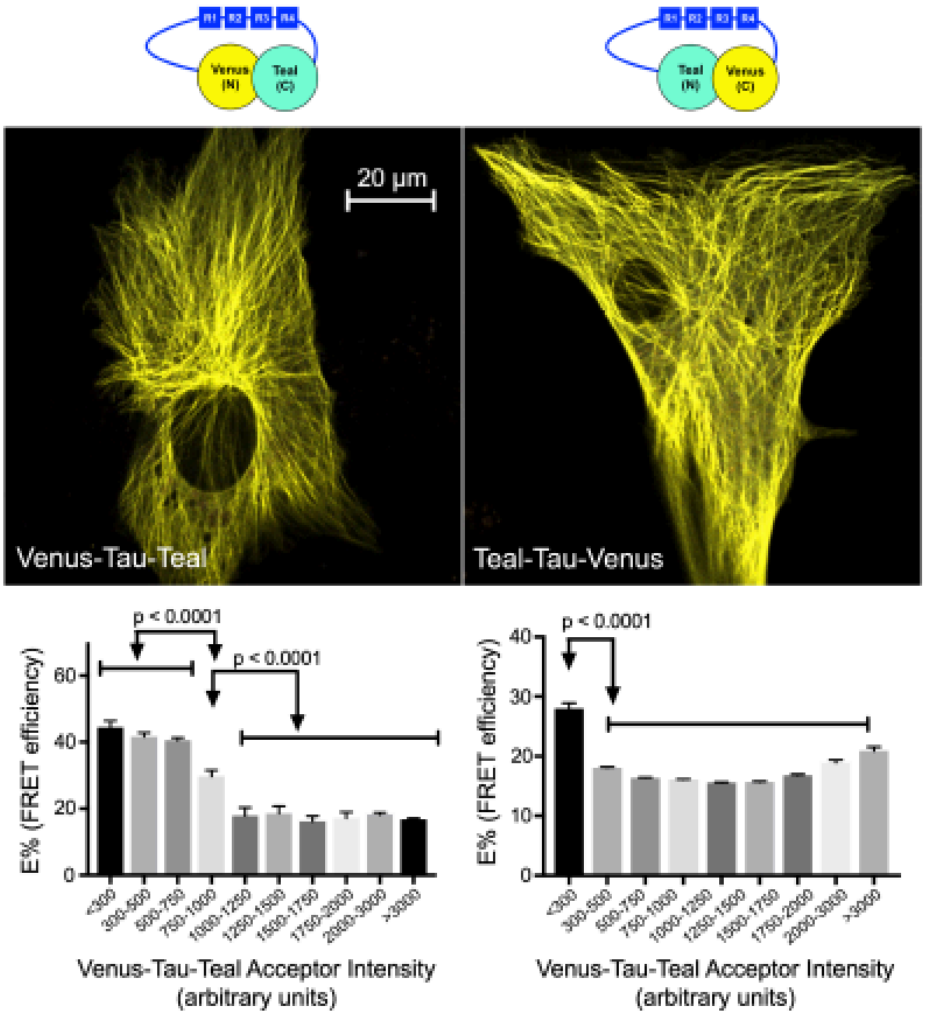

Fig. 3. Venus-Tau-Teal is superior to Teal-Tau-Venus for detecting intramolecular FRET uncompromised by aggregation effects. Venus-Tau-Teal and Teal-Tau-Venus both target to microtubules and show differing dependence of FRET efficiency (E%) on fluorescent fusion protein concentration. Venus-Tau-Teal, but not Teal-Tau-Venus, shows a broad range of E% independent of increasing acceptor (Venus) intensity (up to 750 arbitrary intensity units). FRET within that Venus intensity range was therefore judged to be predominantly intramolecular, and Venus-Tau-Teal was used as the Tau conformation biosensor for all subsequent experiments. To minimize FRET signal contamination caused by Venus-Tau-Teal aggregation, we restricted subsequent observations to the low end of the range in which E% is independent of Venus intensity (correlated to a photon count of less than ~500 arbitrary intensity units).

Bar graphs represent the merged data of 6 fields of view per experiment, repeated in 4 biological replicates with their standard errors of the mean. Statistical significance was determined by one-way ANOVA with Tukey's post-hoc test for multiple comparisons. Standard errors calculated by Prism column statistics.

Figure 4

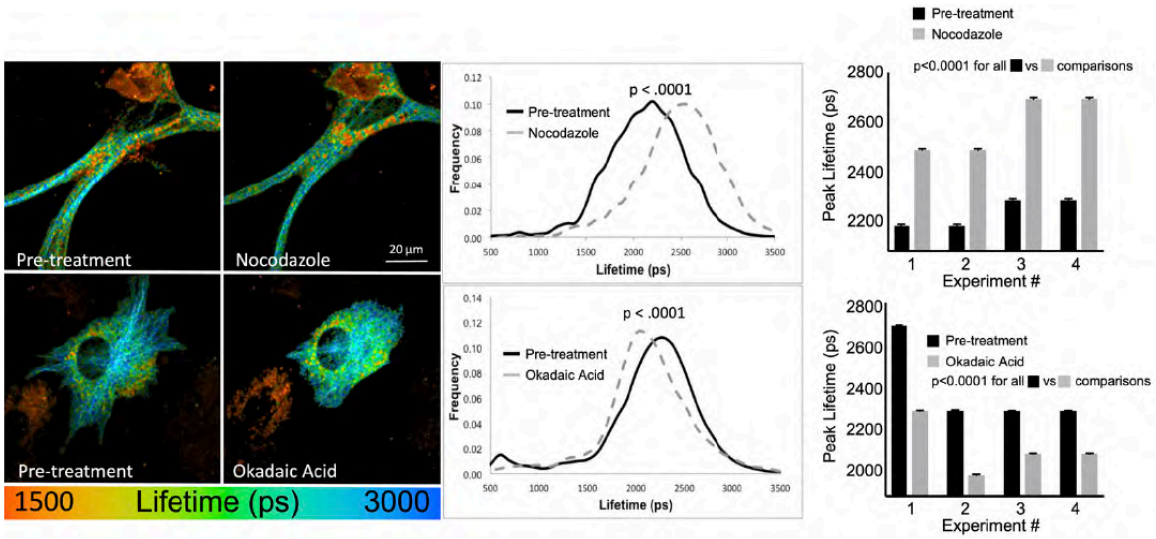

Fig. 4. Modulation of fluorescence lifetime by perturbation of microtubules and protein phosphorylation. CV-1 cells expressing Venus-Tau-Teal were treated on stage for 1 hour with 1μM Nocodazole or Okadaic Acid (OA). Middle panels show the results of a single experiment with distributions compared by the Kolmogorov-Smirnov test. Right panels show a summary of the peak lifetime results of 4 separate experiments.

Figure 5

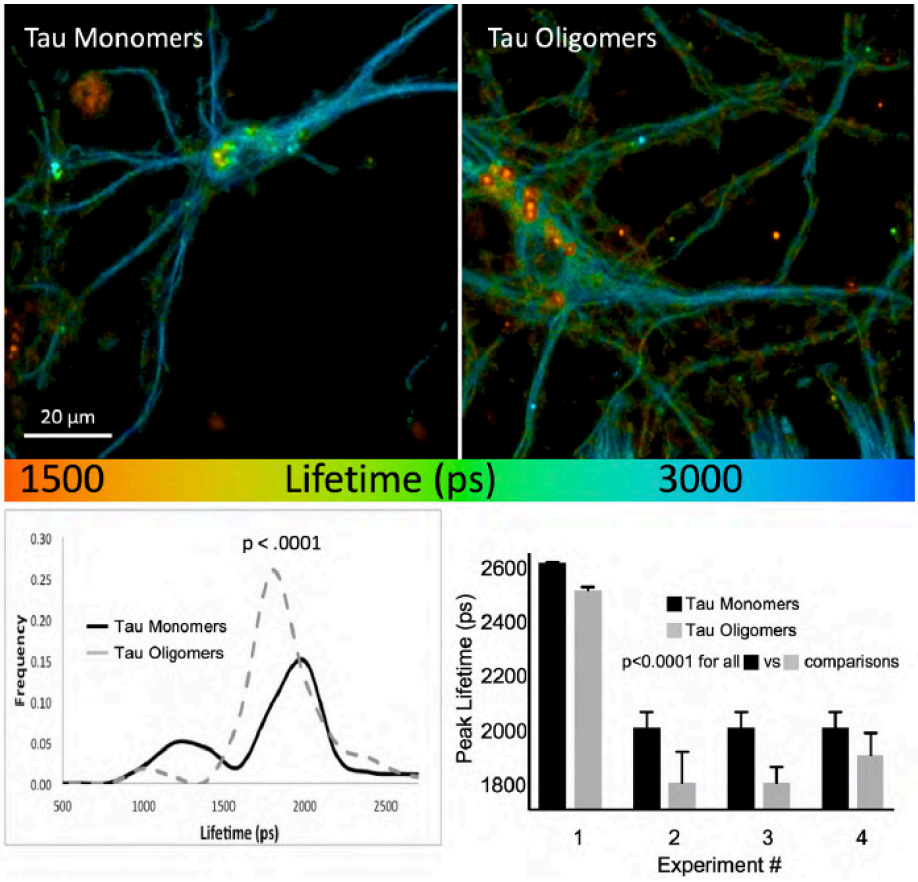

Fig. 5. Venus-Tau-Teal is sensitive to Tau oligomers. Primary cortical mouse brain neurons were treated with human 2N4R Tau monomers or oligomers at a total Tau concentration of 250 nM for 18 hours. Middle panels show the results of a single experiment with distributions compared by the Kolmogorov-Smirnov test. Right panels show a summary of the peak lifetime results of 4 separate experiments.

Figure 6

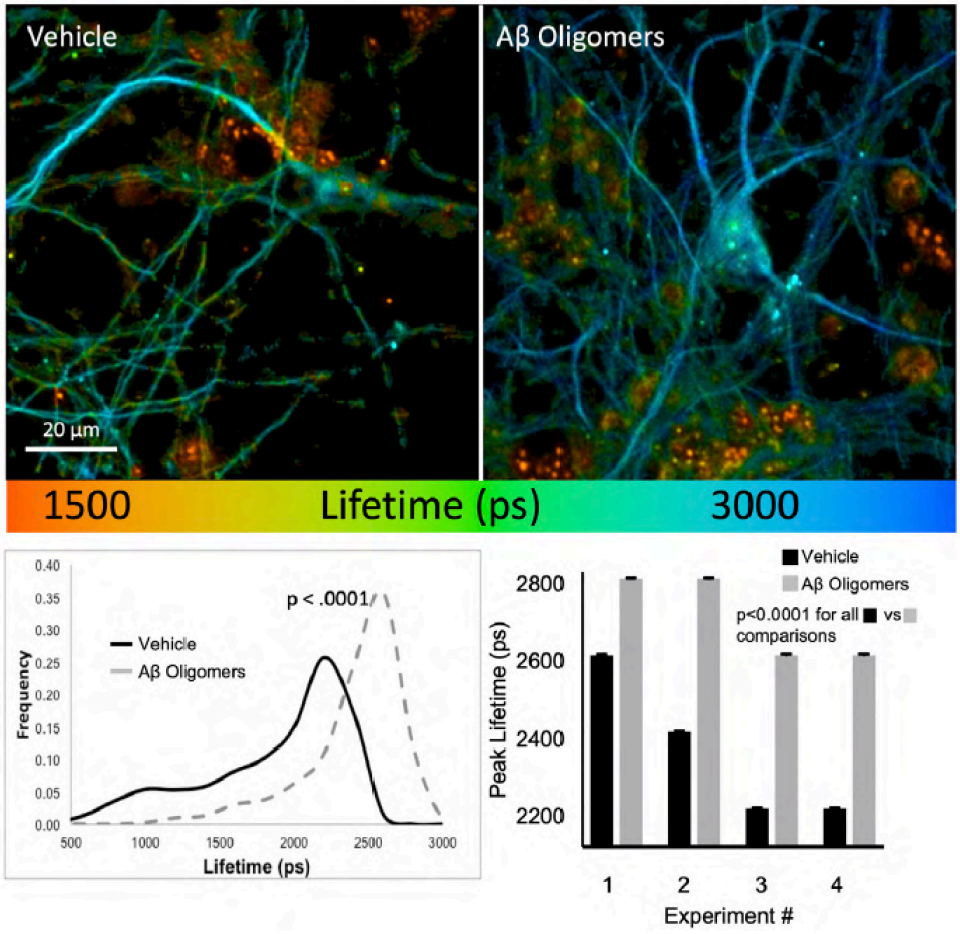

Fig. 6. Venus-Tau-Teal is sensitive to AβOs. Primary cortical mouse brain neurons were treated with vehicle or $A\beta_{1\text{-}42}$ oligomers at a total $A\beta_{1\text{-}42}$ concentration of approximately 1.5 µM for 6 hours. Middle panels show the results of a single experiment with distributions compared by the Kolmogorov-Smirnov test. Right panels show a summary of the peak lifetime results of 4 separate experiments.

Chapter 4: Supplemental data and future work

Chapter 4: Supplemental data and future work

In addition to the results presented above in chapter 3, most of which is accepted pending minor revision to JAD, some other treatments and results showed promise for future work but were too small in magnitude or not yet repeatable enough to warrant publication with the previously described experiments. Among these are a series of experiments testing the effects of taxol on fluorescence lifetime.

Taxol treatments

Like nocodazole, taxol was chosen as a potential treatment due to its established effects on microtubules. Unlike nocodazole which breaks down microtubules, taxol stabilizes microtubules by direct binding to polymerized tubulin. [146,147] Despite its ability to stabilize microtubules, there is evidence that taxol and tau compete for the same binding site on microtubules [135] and taxol treatment causes dissociation of tau from microtubules in Xenopus embryo. [148].

The effect of taxol on fluorescent lifetime was less consistent then other treatments and, though statistically significant, the shift was of small magnitude when a significant effect was seen (Sup. Fig. 3.) As with nocodazole and Aβ treatments, the direction of the shift is consistent with an increase in the distance between donor and acceptor and therefore an opening of the biosensor.

Pathological oligomer timecourses.

Additional experiments were done with various concentrations and time points of tau oligomers. Using treatments of 250nM and 500nM a time course was done between 1 and 18 hours. At 250nM tau oligomers showed no effect on biosensor lifetime at the 1-hour timepoint but significantly shortened lifetime at 6 or 18 hours. At 500nM however a significant shortening of biosensor lifetime was seen as early as 1hr and persisted through 18hrs. (Sup. Fig. 5) This indicates the shift in lifetime due to tau oligomers may be far more rapid than shown by figure 5 at higher treatment concentrations but due to time and cell restraints, more replicates of this experiment would need to be done to confirm this.

The most interesting time course experiment was for the Aβ oligomer treatments. While early time point data described above (6hrs) showed a repeatable increase in lifetime of VtauT, (Figure 6) looking at longer time points yielded an interesting result. When observed at 48hrs the effect of oligomers appears to shift to a shortened lifetime like that seen with tau oligomer treatments (Sup. Fig. 6). This later time point response was difficult to replicate, however. Getting a consistent pool of oligomers is a known difficulty of working with AβO's and so it could be that variations in the oligomer species present could result in the time course of this effect varying with each experiment. It does imply a potential development of the misfolding effect at short time points into an oligomerization effect at longer time points, but additional replicates and longer time point experiments would be necessary to test this hypothesis.

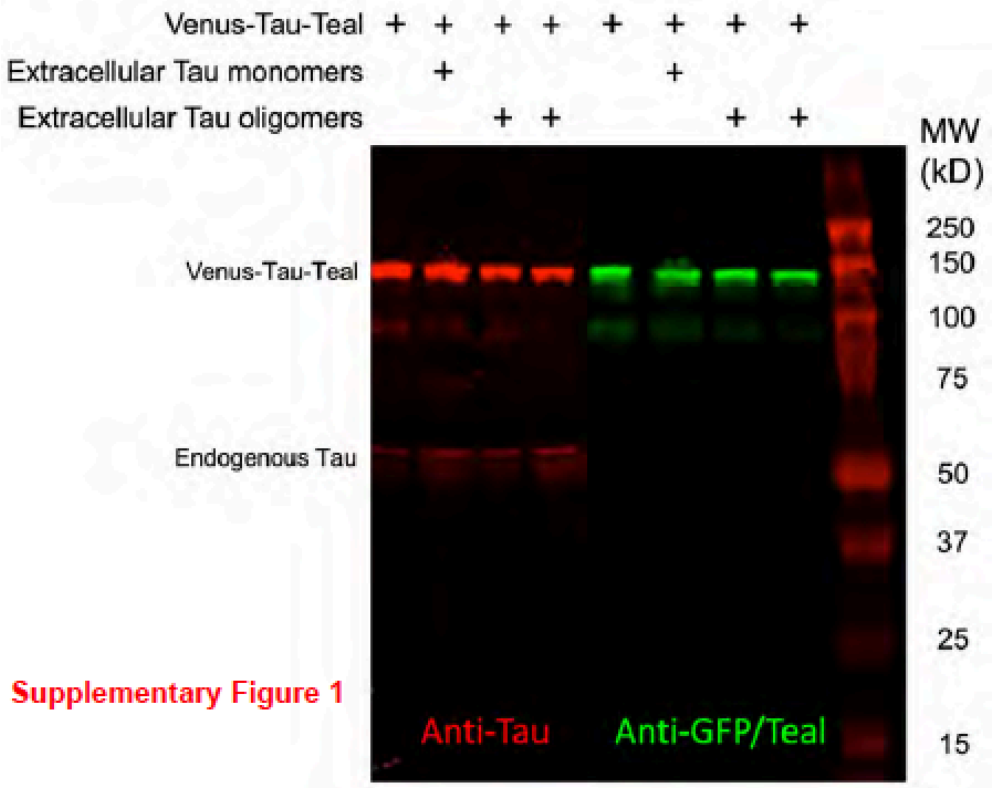

Supplementary Figure 1. Venus-Tau-Teal is not significantly proteolyzed in cultured neurons. Primary mouse cortical neurons that expressed Venus-Tau-Teal were analyzed by western blotting with antibodies to Tau (Tau5) and GFP/Teal (N86).

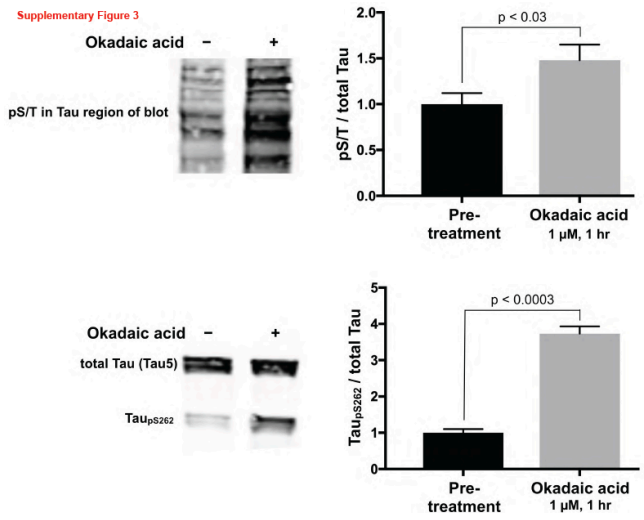

Supplementary Figure 2: Okadaic Acid treatment drives an increase in tau phosphorylation at p262 of the VtauT biosensor VtauT expressing CV1 cells untreated and treated with 1uM okadaic acid for 1 hour. Western blot (left) and quantification normalized to tau5 (right) with pretreatment expression set to 1.

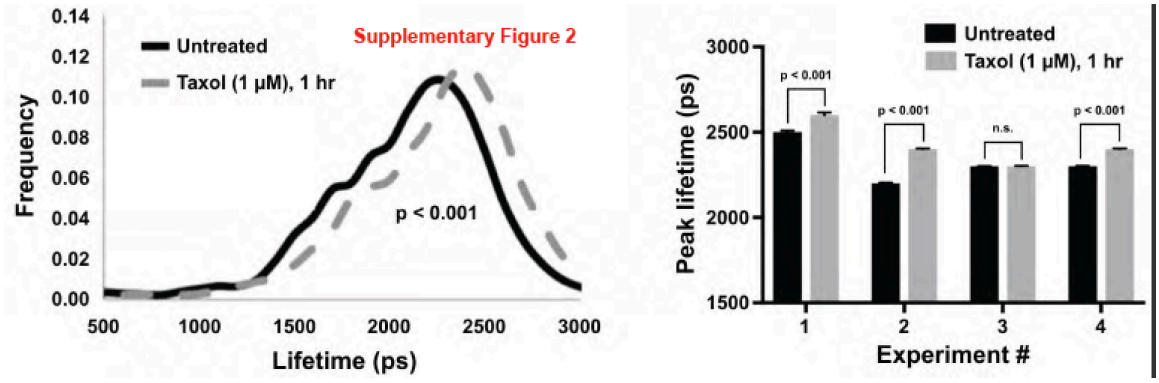

Supplemental Figure 3: Modulation of fluorescence lifetime by perturbation of microtubulbule binding. CV-1 cells expressing Venus-Tau-Teal were treated on stage for 1 hour with 1μM taxol. Middle panel shows the results of a single experiment with distributions compared by the Kolmogorov-Smirnov test. Right panel shows a summary of the peak lifetime results of 4 separate experiments.

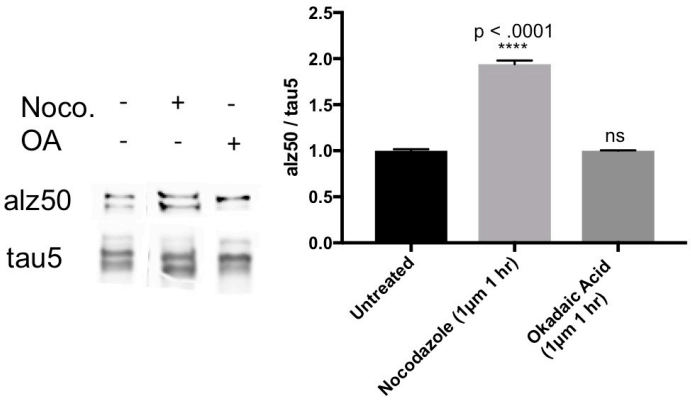

Supplementary Figure 4. VtauT expressing CV1 cells untreated and treated with 1uM okadaic acid or nocodazole for 1 hour. Samples not boiled and probed for Alz50 reactivity. Westerns (left) and quantification (right) bars indicate mean and standard error of n=3 replicates. Quantification analyzed in prism7 by one-way ANOVA and Tukey's post test.

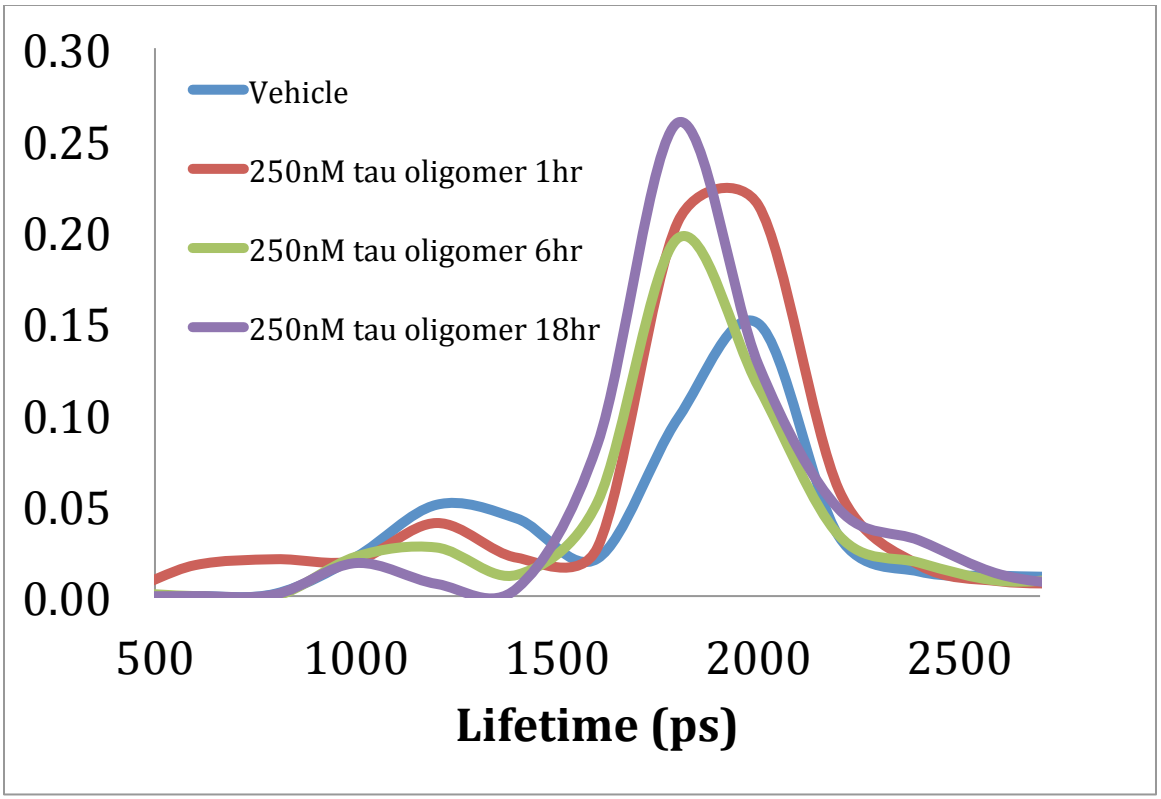

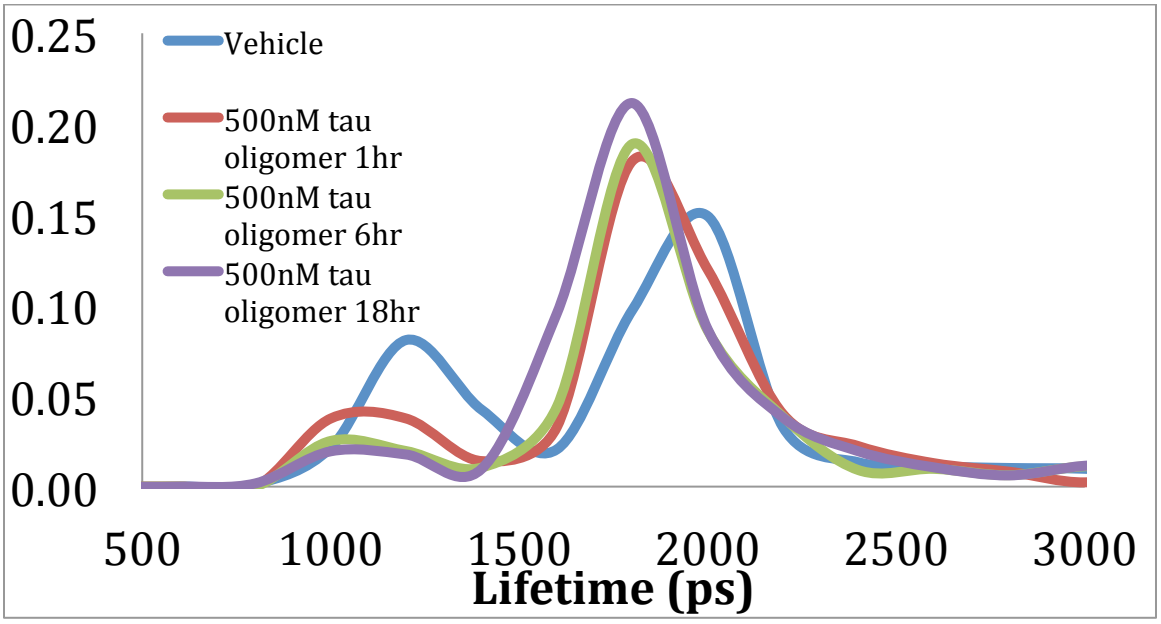

Supplemental Figure 5: Tau oligomer time course. CV-1 cells expressing Venus-Tau-Teal were treated with 250nM (top) or 500nM (bottom) of tau oligomers. Shows the results of a single experiment with distributions compared

by the Kolmogorov-Smirnov test. p<.0001 for all conditions except 250nM at 1 hr.

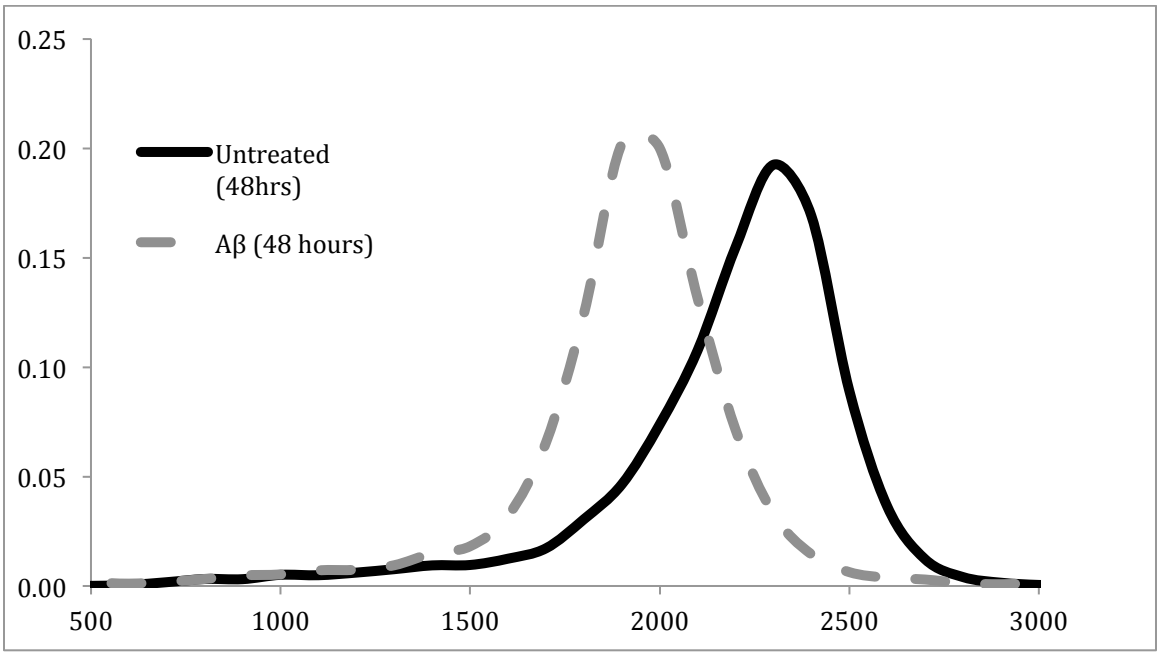

Supplemental Figure 6. AβO oligomer response reverses direction at longer time points (48hrs) Venus-Tau-Teal sensitivity to AβOs seems to shift direction. Primary cortical mouse brain neurons were treated with vehicle or $A\beta_{1-42}$ oligomers at a total Shows panels show the results of a single experiment with distributions compared by the Kolmogorov-Smirnov test p<.0001.

Chapter 5: Prior versions of tau biosensor.

Chapter 5: Prior versions of tau biosensor built

SplitFP background and construct design

As mentioned in the introduction, a previous version of this biosensor was considered aand constructed utilizing a split fluorescent protein design. SplitFP constructs utilize a flourecent protein that is split into two pieces, neither of which are independently fluorescent, however when brought into close proximity fluorescence can be restored indicating protein proximity with a fluorescent signal[149,150]. If successful, a splitFP version of this biosensor would offer a smaller tag load as well as a simplified on/off readout for tau conformation and a simple intensity based analysis which could give it wider applicability as a research tool.

The downside of this kind of biosensor comes from the mixed reports of reversibility. On beginning this body of work it was not clear whether the biosensor would be on or off under basal conditions and if on, whether that switch would be 'stuck' on. There is a significant amount of literature indicating irreversibility of splitFP biosensors [150] but several groups have reported reversibility[151,152] under certain conditions.

To test whether a split tau construct would be on or off under basal conditions and whether it demonstrated any reversibility if on, the pBiFC-VN155(I152L) and pBiFC-VC155 constructs, developed by Chang-Deng Hu, was used to construct an intramolecular splitFP tau biosensor and single labels (Sup. Fig. 7.) Cells expressing the construct appeared to be on under basal conditions, which is consistent with the hairpin folded structure of tau. Upon treatment with

okadaic acid on stage there was some evidence of a rapid reversibility. Treatment with okadaic acid generated a rapid approximately 40% decrease in fluorescent intensity. (Sup. Fig. 8) This potential reversibility was an exciting result but after many permutations of the experiment it was found that the reversibility was unreliable and difficult to replicate. Based on my results, the construct may indeed be reversible under certain conditions or concentrations of expression, but as it was not repeatable or easily controllable, it was determined that a FRET based assay would be preferable for it's known reversibility.

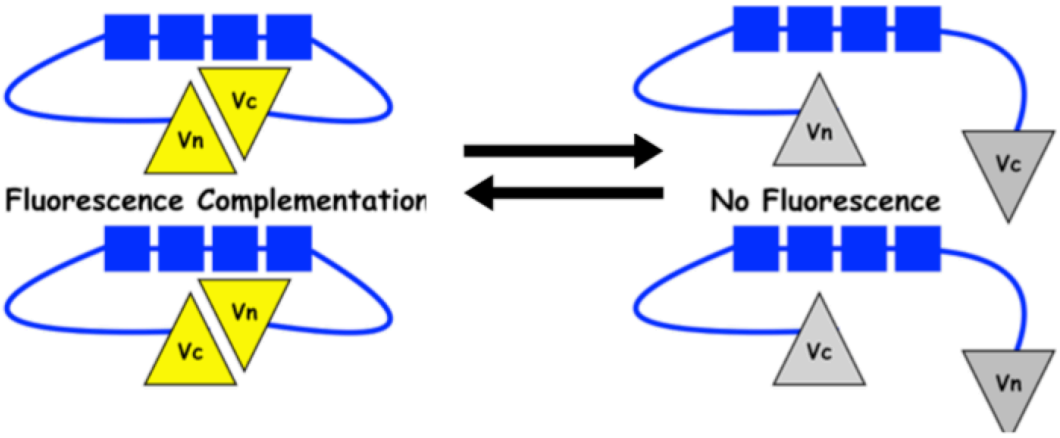

Supplemental Figure 7: Construct design of splitFP based intramolecular tau biosensor.

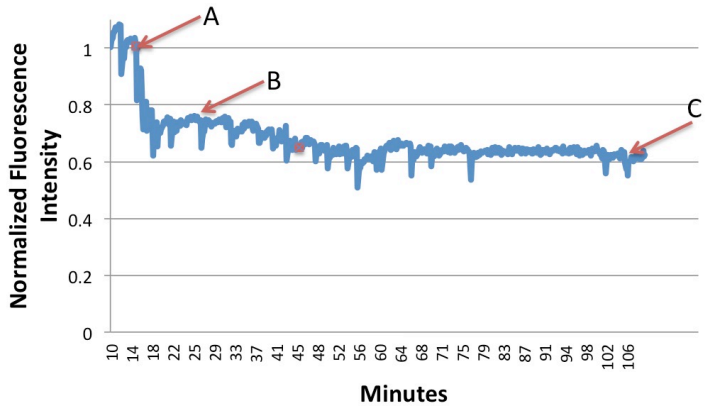

WT neuron culture infected with vntvc lentivirus.

Treated with 50nM okadaic acid at 15 minutes (first arrow)
washed out after 30 minutes

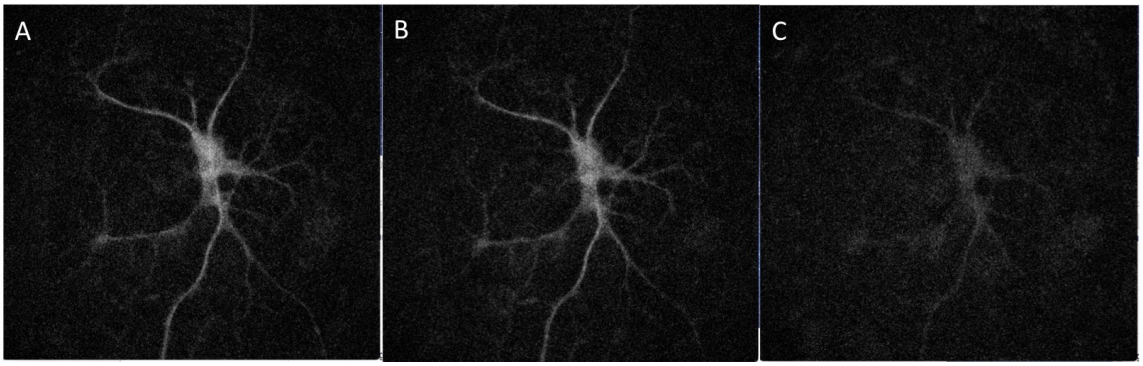

Supplemental Figure 8: WT neurons expressing VN-tau-VC treated with okadaic acid aand then washed out at 30 minutes. Arrows indicate the timepoints of the images below.

Chapter 6: Discussion

Chapter 6: Discussion

Tau misfolding and aggregation underlie the pathogenesis of AD and non-Alzheimer's tauopathies, such as progressive supranuclear palsy, Pick's disease, Parkinson's disease, Huntington's disease and many others. Several methods are well established for detecting aggregated tau, including binding of Congo red,[153] and a variety of antibodies specific for oligomeric or fibrillar Tau [154,155], and PET imaging that can detect neurofibrillary tangles in live patients[156]. In contrast, methods to detect Tau conformational changes that are thought to precede and promote Tau aggregation are far more limited. Two monoclonal antibodies, Alz50 and MC-1, recognize similar discontinuous epitopes that comprise regions of Tau near its N-terminal and within its microtubule-binding repeat region[113,114]. The Alz50 and MC-1 epitopes are infrequently detected in normal brain, and Alz50 and MC-1 immunoreactivity are thought to represent a seminal step in the conversion of normal Tau to pathogenic Tau. The utility of Alz50 and MC-1 is limited, however, to examination of fixed cells and tissues.

Here we describe a new fluorescence-based biosensor, Venus-Tau-Teal, that can detect Tau conformational changes in live cells. Venus-Tau-Teal can discriminate the Tau paperclip/hairpin conformation, in which the N- and C-termini are located in close proximity to each other and to the microtubule-binding repeat region[115,116], from an unfolded conformation in which the Tau N- and C-termini have dissociated. By expressing this biosensor in CV-1 cell fibroblasts and primary mouse cortical neurons, we gathered evidence that the

paperclip/hairpin conformation predominates on microtubule-associated Tau, and is sensitive to a variety of experimental perturbations.

This study represents a refinement of prior work that described a similar biosensor, ECFP-Tau-EYFP, based on human 0N4R Tau[133]. Besides incorporating a superior FRET donor-acceptor pair [122-124] and a different Tau isoform into Venus-Tau-Teal, as compared to ECFP-0N4R Tau-EYFP, we also defined, and exclusively relied on experimental conditions in which intramolecular FRET was minimally contaminated by intermolecular FRET and other possible complications caused by biosensor aggregation.

This was shown experimentally to be a critical improvement over analysis that do not take into account the possibility of intermolecular FRET. Any FRET based biosensor for folding has the capability to produce a signal from the folding of the sensor, as well as by the clustering of the sensor. In fact, the range of FRET efficiencies (E%) in untreated conditions can vary widely, averaging between 40-50% to as low as 10-15% and those averages themselves hide regions of interest with very high and very low calculated E%. (Fig. 3) As demonstrated in figure 3, it is possible to calculate differences in E% with a threefold difference by no perturbation other than analyzing pixels of an untreated cell and binning by intensity. This variation in calculated E% could easily bias an experimental result if the researcher is not carefully controlling their expression levels of analyzed cells. Additionally, small changes to the design of the construct, as with the switch of the teal and venus fluorophores of this construct, have dramatic effects on how the biosensor responds both to

folding and to aggregation (Fig. 3) This work directly addresses the potential weaknesses of, not only previous tau biosensors but of many biosensors developed to analyze various protein-protein interactions, and that alone is among the more important results in this original work with implications spanning the field of biosensors.

By combining this confirmation sensitive biosensor with a method of analysis which can focus in on the intramolecular signal, this biosensor lends additional evidence that, in its unperturbed state, tau adopts a folded confirmation [115,116] and offers furthermore that it maintains that folded state with bound to microtubules (Fig. 3.) When the microtubule network is broken down by treatment with nocodazole, and when tau is in the presence of taxol which causes it to dissociate from MTs, fluorescent lifetime shifts higher (Fig.4, Sup. Fig. 3), a shift consistent with lower efficiency of energy transfer and with an opening of the biosensor. This is consistent with the decrease in FRET efficiency seen using the 0N4R based biosensor, with the previously mentioned caveat of not taking into account intermolecular FRET [133].

The change in direction of the shift in lifetime after okadaic acid treatment is an interesting result. There are many phosphorylation sites in and around the microtubule binding region that can be abnormally phosphorylated in AD [73,91] and the build up of negative charges in that region could have resulted in an unfolding pattern like we saw with nocodazole. Instead we saw a shift towards lower lifetimes after treatment with okadaic acid (Fig. 3) This may be explained by an oligomerization effect driven by hyperphosphorylation. Depending on the

orientation and clustering patterns of oligomers formed, it would not be surprising for tau to organize in a way that also clusters the donor and receptor intermolecularly, resulting in increased efficiency of energy transfer and decreased lifetime of the biosensor within these clusters/oligomers. There is already evidence in the literature to support the pathway from hyperphosphorylation to oligomerization [157,158]

Additionaly, the disparate reactivities of the biosensor to the conformation sensitive Alz50 is intriguing. The increased reactivity of nocodazole treated biosensor to the Alz50 antibody is consistent with a more open conformation seen in the the lifetime data and suggests a different mechanism is indeed driving the downward shift in lifetime upon okadaic acid treatment. As previously discused, this could be explained by a phosphorylayion-sensitive oligomerization event. The subset of oligomer sensitive antibodies described earlier have not yet confirmed this hypothesis, but these antibodies each are sensitive to only one or a subset of oligomers and are quite sensitive to sample preparation (with the presence of SDS and boiling among the more obvious factors controling whether an oligomer is observable via western blot. A more thorough screening including additional antibodies and varying sample preparation would likely be needed to follow up on this result.

While most of the data presented here focused on the characterization of Venus-Tau-Teal (Figs 1-4), our goal from the start was to develop a Tau conformation biosensor that can discriminate normally folded from pathologically folded Tau. We therefore included in the study experiments that monitored

Venus-Tau-Teal responses to pathogenic extracellular oligomers made from Tau or Aβ, each of which disrupts multiple aspects of neuronal homeostasis [63,72-74,138,140-145]. In agreement with the work of Di Primio and colleagues[133], we found that extracellular Tau oligomers cause increased biosensor FRET (Fig. 5), presumably due to intraneuronal Tau aggregation [72,102] in a manner that reinforces Teal-Venus proximity.

Extracellular AβOs caused the opposite response: lengthened Teal fluorescence lifetime of Venus-Tau-Teal, indicative of Tau unfolding from the paperclip/hairpin conformation (Fig 6). One mechanism by which this might occur involves site-specific Tau phosphorylation by multiple protein kinases activated by AβOs. We have shown that AβOs induce ectopic neuronal cell cycle re-entry, which ironically leads to neuron death, by a mechanism that requires Tau phosphorylation at Y18, S262, S409 and S416 by fyn, mTORC1 (probably indirectly through S6 kinase), protein kinase A and CaMKII, respectively [73,145]. It is therefore possible that phosphorylation at some or all of those sites provokes the conformational change from compact and folded to unfolded.

Regardless of what the mechanism may be, the finding that AβOs cause Tau unfolding emphasizes that biochemical effects of AβOs on Tau, such as phosphorylation, are matched by changes in the physical structure of Tau. It follows naturally that detection of molecular species that block or reduce AβO-induced Tau unfolding might aid discovery of new diagnostic biomarkers and disease-modifying drugs for AD.

Chapter 7: Literature Cited

Literature Cited

[1] Papavramidou N (2018) The ancient history of dementia. *Neurol. Sci.* **39**, 2011–2016.

[2] Berchtold NC, Cotman CW (1998) Evolution in the conceptualization of dementia and Alzheimer's disease: Greco-Roman period to the 1960s. *Neurobiol. Aging* **19**, 173–189.

[3] Wilks S (1864) Clinical Notes on Atrophy of the Brain. *Journal of Mental Science* **10**, 381–392.

[4] Ramirez-Bermudez J (2012) Alzheimer's disease: critical notes on the history of a medical concept. *Arch. Med. Res.* **43**, 595–599.

[5] Näslund J, Schierhorn A, Hellman U, Lannfelt L, Roses AD, Tjernberg LO, Silberring J, Gandy SE, Winblad B, Greengard P (1994) Relative abundance of Alzheimer A beta amyloid peptide variants in Alzheimer disease and normal aging. *Proc. Natl. Acad. Sci. U.S.A.* **91**.

[6] Alzheimer's Association (2018) 2018 Alzheimer's disease facts and figures. *Alzheimer's & Dementia* **14**, 367–429.

[7] Holtzman DM, Morris JC, Goate AM (2011) Alzheimer's disease: the challenge of the second century. *Sci Transl Med* **3**, 77sr1–77sr1.

[8] Hyman BT, Phelps CH, Beach TG, Bigio EH, Cairns NJ, Carrillo MC, Dickson DW, Duyckaerts C, Frosch MP, Masliah E, Mirra SS, Nelson PT, Schneider JA, Thal DR, Thies B, Trojanowski JQ, Vinters HV, Montine TJ (2012) National Institute on Aging–Alzheimer“s Association guidelines for the neuropathologic assessment of Alzheimer”s disease. *Alzheimer's & Dementia* **8**, 1–13.

[9] Association AP (2013) *Diagnostic and statistical manual of mental disorders (DSM-5®)*.

[10] Ball MJ, Murdoch GH (1997) Neuropathological criteria for the diagnosis of Alzheimer's disease: are we really ready yet? *Neurobiol. Aging* **18**, S3–12.

[11] Nunes-Tavares N, Santos LE, Stutz B, Brito-Moreira J, Klein WL, Ferreira ST, de Mello FG (2012) Inhibition of choline acetyltransferase as a mechanism for cholinergic dysfunction induced by amyloid-β peptide oligomers. *Journal of Biological Chemistry* **287**, 19377–19385.

[12] Perry EK, Gibson PH, Blessed G, Perry RH, Tomlinson BE (1977) Neurotransmitter enzyme abnormalities in senile dementia: Choline acetyltransferase and glutamic acid decarboxylase activities in necropsy brain tissue. *Journal of the Neurological Sciences* **34**, 247–265.

[13] Terry AV (2003) The cholinergic hypothesis of age and Alzheimer's disease-related cognitive deficits: recent challenges and their implications for novel drug development. *Journal of Pharmacology and Experimental*.

[14] Davies P, Lancet AMT, 1976 *Selective loss of central cholinergic neurons in Alzheimer's disease*.

[15] Rogawski MA, Wenk GL (2003) The neuropharmacological basis for the use of memantine in the treatment of Alzheimer's disease. *CNS Drug Rev* **9**, 275–308.
[16] Zhang H, Zhang Y-W, Thompson R, Xu H (2011) APP processing in Alzheimer's disease. *Mol Brain* **4**, 3.
[17] Postina RR (2008) A closer look at alpha-secretase. *Curr Alzheimer Res* **5**, 179–186.
[18] Wong PC (2011) Amyloid precursor protein processing and Alzheimer's disease. *Annual review of neuroscience*.
[19] Vassar R, Bennett BD, Babu-Khan S, Kahn S, Mendiaz EA, Denis P, Teplow DB, Ross S, Amarante P, Loeloff R, Luo Y, Fisher S, Fuller J, Edenson S, Lile J, Jarosinski MA, Biere AL, Curran E, Burgess T, Louis JC, Collins F, Treanor J, Rogers G, Citron M (1999) Beta-secretase cleavage of Alzheimer's amyloid precursor protein by the transmembrane aspartic protease BACE. *Science* **286**.
[20] Shin J, Yu S-B, Yu UY, Jo SA, Ahn J-H (2010) Swedish mutation within amyloid precursor protein modulates global gene expression towards the pathogenesis of Alzheimer's disease. *BMB Rep* **43**, 704–709.
[21] Jonsson TT, Atwal JKJ, Steinberg SS, Snaedal JJ, Jonsson PVP, Bjornsson SS, Stefansson HH, Sulem PP, Gudbjartsson DD, Maloney JJ, Hoyte KK, Gustafson AA, Liu YY, Lu YY, Bhangale TT, Graham RRR, Huttenlocher JJ, Bjornsdottir GG, Andreassen OAO, Jönsson EGE, Palotie AA, Behrens TWT, Magnusson OTO, Kong AA, Thorsteinsdottir UU, Watts RJR, Stefansson KK (2012) A mutation in APP protects against Alzheimer's disease and age-related cognitive decline. *Nature* **488**, 96–99.
[22] Prasher VP, Farrer MJ, Kessling AM, Fisher EM, West RJ, Barber PC, Butler AC (1998) Molecular mapping of Alzheimer-type dementia in Down's syndrome. *Ann. Neurol.* **43**.
[23] Hanger DP, Brion JP, Gallo JM, Cairns NJ, Luthert PJ, Anderton BH (1991) Tau in Alzheimer“s disease and Down”s syndrome is insoluble and abnormally phosphorylated. *Biochem. J.* **275 (Pt 1)**, 99–104.
[24] Tokuda T, Fukushima T, Ikeda S, Sekijima Y, Shoji S, Yanagisawa N, Tamaoka A (1997) Plasma levels of amyloid beta proteins Abeta1-40 and Abeta1-42(43) are elevated in Down's syndrome. *Ann. Neurol.* **41**.
[25] Hardy J, Allsop D (1991) Amyloid deposition as the central event in the aetiology of Alzheimer's disease. *Trends Pharmacol. Sci.* **12**, 383–388.
[26] Hardy J, Selkoe DJ (2002) The amyloid hypothesis of Alzheimer's disease: progress and problems on the road to therapeutics. *Science* **297**.
[27] Selkoe DJ (2000) Toward a comprehensive theory for Alzheimer“s disease. Hypothesis: Alzheimer”s disease is caused by the cerebral accumulation and cytotoxicity of amyloid beta-protein. *Annals of the*

New York Academy of Sciences **924**.

[28] Bekris LM, Yu C-E, Bird TD, Tsuang DW (2010) Review Article: Genetics of Alzheimer Disease:. *Journal of Geriatric Psychiatry and Neurology* **23**, 213–227.

[29] Goate A, Chartier-Harlin MC, Mullan M, Brown J, Crawford F, Fidani L, Giuffra L, Haynes A, Irving N, James L (1991) Segregation of a missense mutation in the amyloid precursor protein gene with familial Alzheimer's disease. *Nature* **349**, 704–706.

[30] Selkoe DJ, Wolfe MS (2007) Presenilin: running with scissors in the membrane. *Cell* **131**.

[31] Li N-M, Liu K-F, Qiu Y-J, Zhang H-H, Nakanishi H, Qing H (2019) Mutations of beta-amyloid precursor protein alter the consequence of Alzheimer's disease pathogenesis. *Neural Regen Res* **14**, 658–665.

[32] Pauwels K, Williams TL, Morris KL, Jonckheere W, Vandersteen A, Kelly G, Schymkowitz J, Rousseau F, Pastore A, Serpell LC, Broersen K (2012) Structural Basis for Increased Toxicity of Pathological Aβ42:Aβ40 Ratios in Alzheimer Disease. *Journal of Biological Chemistry* **287**, 5650–5660.

[33] Hebert LE, Weuve J, Scherr PA, Evans DA (2013) Alzheimer disease in the United States (2010–2050) estimated using the 2010 census. *Neurology* **80**, 1778–1783.

[34] Marioni RE, Harris SE, Zhang Q, McRae AF, Hagenaars SP, Hill WD, Davies G, Ritchie CW, Gale CR, Starr JM, Goate AM, Porteous DJ, Yang J, Evans KL, Deary IJ, Wray NR, Visscher PM (2018) GWAS on family history of Alzheimer's disease. *Transl Psychiatry* **8**, 99.

[35] Kunkle BW, Grenier-Boley B, Sims R, Bis JC, Damotte V, Naj AC, Boland A, Vronskaya M, van der Lee SJ, Amlie-Wolf A, Bellenguez C, Frizatti A, Chouraki V, Martin ER, Sleegers K, Badarinarayan N, Jakobsdottir J, Hamilton-Nelson KL, Moreno-Grau S, Olaso R, Raybould R, Chen Y, Kuzma AB, Hiltunen M, Morgan T, Ahmad S, Vardarajan BN, Epelbaum J, Hoffmann P, Boada M, Beecham GW, Garnier J-G, Harold D, Fitzpatrick AL, Valladares O, Moutet M-L, Gerrish A, Smith AV, Qu L, Bacq D, Denning N, Jian X, Zhao Y, Del Zompo M, Fox NC, Choi S-H, Mateo I, Hughes JT, Adams HH, Malamon J, Sanchez-Garcia F, Patel Y, Brody JA, Dombroski BA, Naranjo MCD, Daniilidou M, Eiriksdottir G, Mukherjee S, Wallon D, Uphill J, Aspelund T, Cantwell LB, Garzia F, Galimberti D, Hofer E, Butkiewicz M, Fin B, Scarpini E, Sarnowski C, Bush WS, Meslage S, Kornhuber J, White CC, Song Y, Barber RC, Engelborghs S, Sordon S, Voijnovic D, Adams PM, Vandenberghe R, Mayhaus M, Cupples LA, Albert MS, De Deyn PP, Gu W, Himali JJ, Beekly D, Squassina A, Hartmann AM, Orellana A, Blacker D, Rodriguez-Rodriguez E, Lovestone S, Garcia ME, Doody RS, Munoz-Fernadez C, Sussams R, Lin H, Fairchild TJ, Benito YA, Holmes C, Karamujić-Čomić H, Frosch MP, Thonberg H, Maier W, Roschupkin G, Ghetti B, Giedraitis V, Kawalia A, Li S, Huebinger RM, Kilander L, Moebus S, Hernández

I, Kamboh MI, Brundin R, Turton J, Yang Q, Katz MJ, Concari L, Lord J, Beiser AS, Keene CD, Helisalmi S, Kloszewska I, Kukull WA, Koivisto AM, Lynch A, Tarraga L, Larson EB, Haapasalo A, Lawlor B, Mosley TH, Lipton RB, Solfrizzi V, Gill M, Longstreth WT, Montine TJ, Frisardi V, Diez-Fairen M, Rivadeneira F, Petersen RC, Deramecourt V, Alvarez I, Salani F, Ciaramella A, Boerwinkle E, Reiman EM, Fievet N, Rotter JI, Reisch JS, Hanon O, Cupidi C, Andre Uitterlinden AG, Royall DR, Dufouil C, Maletta RG, de Rojas I, Sano M, Brice A, Cecchetti R, George-Hyslop PS, Ritchie K, Tsolaki M, Tsuang DW, Dubois B, Craig D, Wu C-K, Soininen H, Avramidou D, Albin RL, Fratiglioni L, Germanou A, Apostolova LG, Keller L, Koutroumani M, Arnold SE, Panza F, Gkatzima O, Asthana S, Hannequin D, Whitehead P, Atwood CS, Caffarra P, Hampel H, Quintela I, Carracedo Á, Lannfelt L, Rubinsztein DC, Barnes LL, Pasquier F, Frölich L, Barral S, McGuinness B, Beach TG, Johnston JA, Becker JT, Passmore P, Bigio EH, Schott JM, Bird TD, Warren JD, Boeve BF, Lupton MK, Bowen JD, Proitsi P, Boxer A, Powell JF, Burke JR, Kauwe JSK, Burns JM, Mancuso M, Buxbaum JD, Bonuccelli U, Cairns NJ, McQuillin A, Cao C, Livingston G, Carlson CS, Bass NJ, Carlsson CM, Hardy J, Carney RM, Bras J, Carrasquillo MM, Guerreiro R, Allen M, Chui HC, Fisher E, Masullo C, Crocco EA, DeCarli C, Bisceglio G, Dick M, Ma L, Duara R, Graff-Radford NR, Evans DA, Hodges A, Faber KM, Scherer M, Fallon KB, Riemenschneider M, Fardo DW, Heun R, Farlow MR, Kölsch H, Ferris S, Leber M, Foroud TM, Heuser I, Galasko DR, Giegling I, Gearing M, Hüll M, Geschwind DH, Gilbert JR, Morris J, Green RC, Mayo K, Growdon JH, Feulner T, Hamilton RL, Harrell LE, Drichel D, Honig LS, Cushion TD, Huentelman MJ, Hollingworth P, Hulette CM, Hyman BT, Marshall R, Jarvik GP, Meggy A, Abner E, Menzies GE, Jin L-W, Leonenko G, Real LM, Jun GR, Baldwin CT, Grozeva D, Karydas A, Russo G, Kaye JA, Kim R, Jessen F, Kowall NW, Vellas B, Kramer JH, Vardy E, LaFerla FM, Jöckel K-H, Lah JJ, Dichgans M, Leverenz JB, Mann D, Levey AI, Pickering-Brown S, Lieberman AP, Klopp N, Lunetta KL, Wichmann H-E, Lyketsos CG, Morgan K, Marson DC, Brown K, Martiniuk F, Medway C, Mash DC, Nöthen MM, Masliah E, Hooper NM, McCormick WC, Daniele A, McCurry SM, Bayer A, McDavid AN, Gallacher J, McKee AC, van den Bussche H, Mesulam M, Brayne C, Miller BL, Riedel-Heller S, Miller CA, Miller JW, Al-Chalabi A, Morris JC, Shaw CE, Myers AJ, Wiltfang J, O'Bryant S, Olichney JM, Alvarez V, Parisi JE, Singleton AB, Paulson HL, Collinge J, Perry WR, Mead S, Peskind E, Cribbs DH, Rossor M, Pierce A, Ryan NS, Poon WW, Nacmias B, Potter H, Sorbi S, Quinn JF, Sacchinelli E, Raj A, Spalletta G, Raskind M, Caltagirone C, Bossù P, Orfei MD, Reisberg B, Clarke R, Reitz C, Smith AD, Ringman JM, Warden D, Roberson ED, Wilcock G, Rogaeva E, Bruni AC, Rosen HJ, Gallo M, Rosenberg RN, Ben-Shlomo Y, Sager MA,

Mecocci P, Saykin AJ, Pastor P, Cuccaro ML, Vance JM, Schneider JA, Schneider LS, Slifer S, Seeley WW, Smith AG, Sonnen JA, Spina S, Stern RA, Swerdlow RH, Tang M, Tanzi RE, Trojanowski JQ, Troncoso JC, Van Deerlin VM, Van Eldik LJ, Vinters HV, Vonsattel JP, Weintraub S, Welsh-Bohmer KA, Wilhelmsen KC, Williamson J, Wingo TS, Woltjer RL, Wright CB, Yu C-E, Yu L, Saba Y, Alzheimer Disease Genetics Consortium (ADGC),, European Alzheimer's Disease Initiative (EADI),, Cohorts for Heart and Aging Research in Genomic Epidemiology Consortium (CHARGE),, Genetic and Environmental Risk in AD/Defining Genetic, Polygenic and Environmental Risk for Alzheimer's Disease Consortium (GERAD/PERADES),, Pilotto A, Bullido MJ, Peters O, Crane PK, Bennett D, Bosco P, Coto E, Boccardi V, De Jager PL, Lleo A, Warner N, Lopez OL, Ingelsson M, Deloukas P, Cruchaga C, Graff C, Gwilliam R, Fornage M, Goate AM, Sanchez-Juan P, Kehoe PG, Amin N, Ertekin-Taner N, Berr C, Debette S, Love S, Launer LJ, Younkin SG, Dartigues J-F, Corcoran C, Ikram MA, Dickson DW, Nicolas G, Campion D, Tschanz J, Schmidt H, Hakonarson H, Clarimon J, Munger R, Schmidt R, Farrer LA, Van Broeckhoven C, C O'Donovan M, DeStefano AL, Jones L, Haines JL, Deleuze J-F, Owen MJ, Gudnason V, Mayeux R, Escott-Price V, Psaty BM, Ramirez A, Wang L-S, Ruiz A, van Duijn CM, Holmans PA, Seshadri S, Williams J, Amouyel P, Schellenberg GD, Lambert J-C, Pericak-Vance MA (2019) Genetic meta-analysis of diagnosed Alzheimer's disease identifies new risk loci and implicates Aβ, tau, immunity and lipid processing. *Nat. Genet.* **51**, 414–430.

[36] Bis JC, Jian X, Kunkle BW, Chen Y, Hamilton-Nelson KL, Bush WS, Salerno WJ, Lancour D, Ma Y, Renton AE, Marcora E, Farrell JJ, Zhao Y, Qu L, Ahmad S, Amin N, Amouyel P, Beecham GW, Below JE, Campion D, Charbonnier C, Chung J, Crane PK, Cruchaga C, Cupples LA, Dartigues J-F, Debette S, Deleuze J-F, Fulton L, Gabriel SB, Genin E, Gibbs RA, Goate A, Grenier-Boley B, Gupta N, Haines JL, Havulinna AS, Helisalmi S, Hiltunen M, Howrigan DP, Ikram MA, Kaprio J, Konrad J, Kuzma A, Lander ES, Lathrop M, Lehtimäki T, Lin H, Mattila K, Mayeux R, Muzny DM, Nasser W, Neale B, Nho K, Nicolas G, Patel D, Pericak-Vance MA, Perola M, Psaty BM, Quenez O, Rajabli F, Redon R, Reitz C, Remes AM, Salomaa V, Sarnowski C, Schmidt H, Schmidt M, Schmidt R, Soininen H, Thornton TA, Tosto G, Tzourio C, van der Lee SJ, van Duijn CM, Vardarajan B, Wang W, Wijsman E, Wilson RK, Witten D, Worley KC, Zhang X, Alzheimer's Disease Sequencing Project, Bellenguez C, Lambert J-C, Kurki MI, Palotie A, Daly M, Boerwinkle E, Lunetta KL, DeStefano AL, Dupuis J, Martin ER, Schellenberg GD, Seshadri S, Naj AC, Fornage M, Farrer LA (2018) Whole exome sequencing study identifies novel rare and common Alzheimer's-Associated variants involved in immune response and transcriptional regulation. *Mol. Psychiatry* **9**, e94661.

[37] Raber J, Huang Y, Ashford JW (2004) ApoE genotype accounts for the vast majority of AD risk and AD pathology. *Neurobiol. Aging* **25**, 641–650.

[38] Verghese PB, Castellano JM, Holtzman DM (2011) Apolipoprotein E in Alzheimer's disease and other neurological disorders. *The Lancet Neurology* **10**, 241–252.

[39] Holtzman DM, Herz J, Bu G (2012) Apolipoprotein e and apolipoprotein e receptors: normal biology and roles in Alzheimer disease. *Cold Spring Harb Perspect Med* **2**, a006312.

[40] Jiang Q, Lee CY, Mandrekar S, Wilkinson B (2008) ApoE promotes the proteolytic degradation of Aβ. *Neuron*.

[41] Cramer PE, Cirrito JR, Wesson DW, Lee CY, Karlo JC, Zinn AE, Casali BT, Restivo JL, Goebel WD, James MJ, Brunden KR, Wilson DA, Landreth GE (2012) ApoE-directed therapeutics rapidly clear β-amyloid and reverse deficits in AD mouse models. *Science* **335**.

[42] Mouchard A, Boutonnet M-C, Mazzocco C, Biendon N, Macrez N, Neuro-CEB Neuropathology Network (2019) ApoE-fragment/Aβ heteromers in the brain of patients with Alzheimer's disease. *Sci Rep* **9**, 3989.

[43] Hashimoto T, Serrano-Pozo A, Hori Y, Adams KW, Takeda S, Banerji AO, Mitani A, Joyner D, Thyssen DH, Bacskai BJ, Frosch MP, Spires-Jones TL, Finn MB, Holtzman DM, Hyman BT (2012) Apolipoprotein E, especially apolipoprotein E4, increases the oligomerization of amyloid β peptide. *Journal of Neuroscience* **32**, 15181–15192.

[44] Chen Y, Durakoglugil MS, Xian X, Herz J (2010) ApoE4 reduces glutamate receptor function and synaptic plasticity by selectively impairing ApoE receptor recycling. *Proc. Natl. Acad. Sci. U.S.A.* **107**, 12011–12016.

[45] Fleminger S, Oliver DL, Lovestone S (2003) Head injury as a risk factor for Alzheimer's disease: the evidence 10 years on; a partial replication. *Journal of Neurology*.

[46] Plassman BL, Havlik RJ, Steffens DC, Helms MJ (2000) Documented head injury in early adulthood and risk of Alzheimer's disease and other dementias. *Neurology*.

[47] Johnson VE, Stewart W, Smith DH (2010) Traumatic brain injury and amyloid-β pathology: a link to Alzheimer's disease? *Nature Reviews Neuroscience* **11**, 361–370.

[48] Raby CA, Morganti Kossmann MC (1998) Traumatic Brain Injury Increases β‐Amyloid Peptide 1‐42 in Cerebrospinal Fluid. *Journal of*.

[49] Marklund N, Blennow K, Zetterberg H, Ronne-Engström E, Enblad P, Hillered L (2009) Monitoring of brain interstitial total tau and beta amyloid proteins by microdialysis in patients with traumatic brain injury. *J. Neurosurg.* **110**, 1227–1237.

[50] Anstey KJ, Sanden von C, Salim A, O'Kearney R (2007) Smoking as a risk factor for dementia and cognitive decline: a meta-analysis of prospective studies. *Am. J. Epidemiol.* **166**, 367–378.

[51] Stirland LE, O'Shea CI, Russ TC (2018) Passive smoking as a risk factor for dementia and cognitive impairment: systematic review of observational studies. *Int Psychogeriatr* **30**, 1177–1187.
[52] Rönnemaa E, Zethelius B, Lannfelt L, Kilander L (2011) Vascular risk factors and dementia: 40-year follow-up of a population-based cohort. *Dement Geriatr Cogn Disord* **31**, 460–466.
[53] Kingwell K (2011) Overweight or obesity during midlife is associated with late-life dementia. *Nat Rev Neurol* **7**, 299–299.
[54] Benilova I, Karran E, De Strooper B (2012) The toxic Aβ oligomer and Alzheimer's disease: an emperor in need of clothes. *Nat. Neurosci.* **15**.
[55] Wujek JR, Dority MD, Frederickson RC, Brunden KR (1996) Deposits of A beta fibrils are not toxic to cortical and hippocampal neurons in vitro. *Neurobiol. Aging* **17**.
[56] Dodart J-C, Bales KR, Gannon KS, Greene SJ, DeMattos RB, Mathis C, DeLong CA, Wu S, Wu X, Holtzman DM, Paul SM (2002) Immunization reverses memory deficits without reducing brain Abeta burden in Alzheimer's disease model. *Nat. Neurosci.* **5**.
[57] Röskam S, Neff F, Schwarting R, Bacher M, Dodel R (2010) APP transgenic mice: the effect of active and passive immunotherapy in cognitive tasks. *Neurosci Biobehav Rev* **34**, 487–499.
[58] Pike CJ, Walencewicz AJ, Glabe CG, Cotman CW (1991) In vitro aging of beta-amyloid protein causes peptide aggregation and neurotoxicity. *Brain Res.* **563**.
[59] Giuffrida ML, Caraci F, Pignataro B, Cataldo S, de Bona P, Bruno V, Molinaro G, Pappalardo G, Messina A, Palmigiano A, Garozzo D, Nicoletti F, Rizzarelli E, Copani A (2009) Beta-amyloid monomers are neuroprotective. *J. Neurosci.* **29**.
[60] Kayed R, Head E, Thompson JL, McIntire TM, Milton SC, Cotman CW, Glabe CG (2003) Common structure of soluble amyloid oligomers implies common mechanism of pathogenesis. *Science* **300**.
[61] Oddo S, Caccamo A, Tran L, Lambert MP, Glabe CG, Klein WL, LaFerla FM (2006) Temporal profile of amyloid-beta (Abeta) oligomerization in an in vivo model of Alzheimer disease. A link between Abeta and tau pathology. *J. Biol. Chem.* **281**.
[62] McLean CA, Cherny RA, Fraser FW, Fuller SJ, Smith MJ, Beyreuther K, Bush AI, Masters CL (1999) Soluble pool of Abeta amyloid as a determinant of severity of neurodegeneration in Alzheimer's disease. *Ann. Neurol.* **46**.
[63] Walsh DM, Klyubin I, Fadeeva JV, Cullen WK, Anwyl R, Wolfe MS, Rowan MJ, Selkoe DJ (2002) Naturally secreted oligomers of amyloid beta protein potently inhibit hippocampal long-term potentiation in vivo. *Nature* **416**.
[64] Lee VM (2001) Biomedicine. Tauists and beta-aptists united--well almost! *Science* **293**, 1446–1447.
[65] Götz J, Chen F, van Dorpe J, Nitsch RM (2001) Formation of

neurofibrillary tangles in P301l tau transgenic mice induced by Abeta 42 fibrils. *Science* **293**.

[66] Lewis J, Dickson DW, Lin WL, Chisholm L, Corral A, Jones G, Yen SH, Sahara N, Skipper L, Yager D, Eckman C, Hardy J, Hutton M, McGowan E (2001) Enhanced neurofibrillary degeneration in transgenic mice expressing mutant tau and APP. *Science* **293**, 1487–1491.

[67] Roberson ED, Scearce-Levie K, Palop JJ, Yan F, Cheng IH, Wu T, Gerstein H, Yu G-Q, Mucke L (2007) Reducing endogenous tau ameliorates amyloid beta-induced deficits in an Alzheimer's disease mouse model. *Science* **316**, 750–754.

[68] Zempel H, Luedtke J, Kumar Y, Biernat J, Dawson H, Mandelkow E, Mandelkow E-M (2013) oligomers induce synaptic damage via Tau-dependent microtubule severing by TTLL6 and spastin. *EMBO J.* 1–18.

[69] King ME, Kan H-M, Baas PW, Erisir A, Glabe CG, Bloom GS (2006) Tau-dependent microtubule disassembly initiated by prefibrillar beta-amyloid. *J. Cell Biol.* **175**.

[70] Ittner LM, Ke YD, Delerue F, Bi M, Gladbach A, van Eersel J, Wölfing H, Chieng BC, Christie MJ, Napier IA, Eckert A, Staufenbiel M, Hardeman E, Götz J (2010) Dendritic function of tau mediates amyloid-beta toxicity in Alzheimer's disease mouse models. *Cell* **142**, 1–11.

[71] Vossel KA, Xu JC, Fomenko V, Miyamoto T, Suberbielle E, Knox JA, Ho K, Kim DH, Yu G-Q, Mucke L (2015) Tau reduction prevents Aβ-induced axonal transport deficits by blocking activation of GSK3β. *J. Cell Biol.* **209**, 419–433.

[72] Swanson E, Breckenridge L, McMahon L, Som S, McConnell I, Bloom GS (2017) Extracellular Tau Oligomers Induce Invasion of Endogenous Tau into the Somatodendritic Compartment and Axonal Transport Dysfunction. *J. Alzheimers Dis.* **58**, 803–820.

[73] Seward ME, Swanson E, Norambuena A, Reimann A, Cochran JN, Li R, Roberson ED, Bloom GS (2013) Amyloid-β signals through tau to drive ectopic neuronal cell cycle re-entry in Alzheimer's disease. *J Cell Sci* **126**, 1278–1286.

[74] Nussbaum JM, Schilling S, Cynis H, Silva A, Swanson E, Wangsanut T, Tayler K, Wiltgen B, Hatami A, Rönicke R, Reymann K, Hutter-Paier B, Alexandru A, Jagla W, Graubner S, Glabe CG, Demuth H-U, Nussbaum GB (2012) Prion-Like Behavior and Tau-dependent Cytotoxicity of β-Amyloid Oligomers Seeded by Pyroglutamylated β-Amyloid. *Nature* 1–18.

[75] Goedert M, Jakes R (1990) Expression of separate isoforms of human tau protein: correlation with the tau pattern in brain and effects on tubulin polymerization. *EMBO J.* **9**, 4225–4230.

[76] Brandt R, Lee G (1993) Functional organization of microtubule-associated protein tau. Identification of regions which affect

microtubule growth, nucleation, and bundle formation in vitro. *Journal of Biological Chemistry* **268**, 3414–3419.

[77] Morris M, Maeda S, Vossel K, Mucke L (2011) The Many Faces of Tau. *Neuron* **70**, 410–426.

[78] Bergen von M, Barghorn S, Li L, Marx A, Biernat J, Mandelkow EM, Mandelkow E (2001) Mutations of tau protein in frontotemporal dementia promote aggregation of paired helical filaments by enhancing local beta-structure. *Journal of Biological Chemistry* **276**, 48165–48174.

[79] Weingarten MD, Lockwood AH, Hwo SY, Kirschner MW (1975) A protein factor essential for microtubule assembly. *Proc. Natl. Acad. Sci. U.S.A.* **72**, 1858–1862.

[80] Chen J, Kanai Y, Cowan NJ, Hirokawa N (1992) Projection domains of MAP2 and tau determine spacings between microtubules in dendrites and axons. *Nature* **360**, 674–677.

[81] Liu C, Götz J (2013) Profiling murine tau with 0N, 1N and 2N isoform-specific antibodies in brain and peripheral organs reveals distinct subcellular localization, with the 1N isoform being enriched in the nucleus. *PLoS ONE* **8**, e84849.

[82] Maday S, Twelvetrees AE, Moughamian AJ, Holzbaur ELF (2014) Axonal transport: cargo-specific mechanisms of motility and regulation. *Neuron* **84**, 292–309.

[83] Ebneth A, Godemann R, Stamer K, Illenberger S, Trinczek B, Mandelkow E (1998) Overexpression of tau protein inhibits kinesin-dependent trafficking of vesicles, mitochondria, and endoplasmic reticulum: implications for Alzheimer's disease. *J. Cell Biol.* **143**, 777–794.

[84] Dixit R, Ross JL, Goldman YE, Holzbaur ELF (2008) Differential regulation of dynein and kinesin motor proteins by tau. *Science* **319**, 1086–1089.

[85] Mandell JW, Banker GA (1996) A spatial gradient of tau protein phosphorylation in nascent axons. *Journal of Neuroscience* **16**, 5727–5740.

[86] Violet M, Delattre L, Tardivel M, Sultan A, Chauderlier A, Caillierez R, Talahari S, Nesslany F, Lefebvre B, Bonnefoy E, Buée L, Galas M-C (2014) A major role for Tau in neuronal DNA and RNA protection in vivo under physiological and hyperthermic conditions. *Front Cell Neurosci* **8**, 84.

[87] Wang Y, Mandelkow E (2016) Tau in physiology and pathology. *Nature Reviews Neuroscience* **17**, 5–21.

[88] Barghorn S, Zheng-Fischhöfer Q, Ackmann M, Biernat J, Bergen von M, Mandelkow EM, Mandelkow E (2000) Structure, microtubule interactions, and paired helical filament aggregation by tau mutants of frontotemporal dementias. *Biochemistry* **39**, 11714–11721.

[89] Hong M, Zhukareva V, Vogelsberg-Ragaglia V, Wszolek Z, Reed L, Miller BI, Geschwind DH, Bird TD, McKeel D, Goate A, Morris JC,

Wilhelmsen KC, Schellenberg GD, Trojanowski JQ, Lee VM (1998) Mutation-specific functional impairments in distinct tau isoforms of hereditary FTDP-17. *Science* **282**.

[90] Köpke E (1993) Microtubule-associated protein tau. Abnormal phosphorylation of a non-paired helical filament pool in Alzheimer disease. *Journal of Biological Chemistry* **268**, 24374–24384.

[91] Alonso AD, Di Clerico J, Li B, Corbo CP, Alaniz ME, Grundke-Iqbal I, Iqbal K (2010) Phosphorylation of tau at Thr212, Thr231, and Ser262 combined causes neurodegeneration. *Journal of Biological Chemistry* **285**, 30851–30860.

[92] Chu D, Liu F (2018) Pathological Changes of Tau Related to Alzheimer's Disease. *ACS Chem. Neurosci.* acschemneuro.8b00457.

[93] Gong C-X, Singh TJ, Iqbal IG, Iqbal K (1993) Phosphoprotein Phosphatase Activities in Alzheimer Disease Brain. *Journal of Neurochemistry* **61**, 921–927.

[94] Bialojan C, Takai A (1988) Inhibitory effect of a marine-sponge toxin, okadaic acid, on protein phosphatases. Specificity and kinetics. *Biochem. J.* **256**, 283–290.

[95] Prusiner SB (1982) Novel proteinaceous infectious particles cause scrapie. *Science* **216**, 136–144.

[96] Bloom GS, Nussbaum JM, Seward M (2012) Alzheimer's Disease: a Tale of Two Prions

. 1–22.

[97] Braak H, Braak E (1991) Neuropathological stageing of Alzheimer-related changes. *Acta Neuropathol* **82**, 239–259.

[98] Braak H, Del Tredici K (2011) Alzheimer’s pathogenesis: is there neuron-to-neuron propagation? *Acta Neuropathol* **121**, 589–595.

[99] Clavaguera F, Bolmont T, Crowther RA, Abramowski D, Frank S, Probst A, Fraser G, Stalder AK, Beibel M, Staufenbiel M, Jucker M, Goedert M, Tolnay M (2009) Transmission and spreading of tauopathy in transgenic mouse brain. *Nat. Cell Biol.* **11**, 909–913.

[100] Carlson GA, Spires-Jones TL, Hyman BT (2012) Propagation of Tau Pathology in a Model of Early Alzheimer's Disease. *Neuron*.

[101] Liu L, Drouet V, Wu JW, Witter MP, Small SA, Clelland C, Duff K (2012) Trans-synaptic spread of tau pathology in vivo. *PLoS ONE* **7**, e31302.

[102] Frost B, Jacks RL, Diamond MI (2009) Propagation of tau misfolding from the outside to the inside of a cell. *Journal of Biological Chemistry* **284**, 12845–12852.

[103] Mukrasch MD, Bibow S, Korukottu J, Jeganathan S, Biernat J, Griesinger C, Mandelkow E, Zweckstetter M (2009) Structural polymorphism of 441-residue tau at single residue resolution. *PLoS Biol.* **7**, e34.

[104] Lee G, Cowan N, Kirschner M (1988) The primary structure and heterogeneity of tau protein from mouse brain. *Science* **239**, 285–288.

[105] Schweers O, Schönbrunn-Hanebeck E, Marx A, Mandelkow E (1994) Structural studies of tau protein and Alzheimer paired helical filaments show no evidence for beta-structure. *Journal of Biological Chemistry* **269**, 24290–24297.

[106] Jeganathan S, Bergen von M, Mandelkow E-M, Mandelkow E (2008) The natively unfolded character of tau and its aggregation to Alzheimer-like paired helical filaments. *Biochemistry* **47**, 10526–10539.

[107] Goedert M, Jakes R, Spillantini MG, Hasegawa M, Smith MJ, Crowther RA (1996) Assembly of microtubule-associated protein tau into Alzheimer-like filaments induced by sulphated glycosaminoglycans. *Nature* **383**, 550–553.

[108] King ME, Gamblin TC, Kuret J, Binder LI (2000) Differential assembly of human tau isoforms in the presence of arachidonic acid. *Journal of Neurochemistry* **74**, 1749–1757.

[109] KIDD M (1963) Paired helical filaments in electron microscopy of Alzheimer's disease. *Nature* **197**, 192–193.

[110] Bergen von M, Barghorn S, Biernat J, Mandelkow E-M, Mandelkow E (2005) Tau aggregation is driven by a transition from random coil to beta sheet structure. *Biochimica et Biophysica Acta (BBA) - Molecular Basis of Disease* **1739**, 158–166.

[111] Bergen von M, Friedhoff P, Biernat J, Heberle J, Mandelkow EM, Mandelkow E (2000) Assembly of tau protein into Alzheimer paired helical filaments depends on a local sequence motif ((306)VQIVYK(311)) forming beta structure. *Proc. Natl. Acad. Sci. U.S.A.* **97**, 5129–5134.

[112] Berry RW, Abraha A, Lagalwar S, LaPointe N, Gamblin TC, Cryns VL, Binder LI (2003) Inhibition of tau polymerization by its carboxy-terminal caspase cleavage fragment. *Biochemistry* **42**, 8325–8331.

[113] Carmel G, Mager EM, Binder LI, Kuret J (1996) The structural basis of monoclonal antibody Alz50“s selectivity for Alzheimer”s disease pathology. *Journal of Biological Chemistry* **271**, 32789–32795.

[114] Jicha GA, Bowser R, Kazam IG, Davies P (1997) Alz-50 and MC-1, a new monoclonal antibody raised to paired helical filaments, recognize conformational epitopes on recombinant tau. *J. Neurosci. Res.* **48**, 128–132.

[115] Horowitz PM, LaPointe N, Guillozet-Bongaarts AL, Berry RW, Binder LI (2006) N-Terminal Fragments of Tau Inhibit Full-Length Tau Polymerization in Vitro †. *Biochemistry* **45**, 12859–12866.

[116] Jeganathan S, Bergen von M, Brutlach H, Steinhoff H-J, Mandelkow E (2006) Global hairpin folding of tau in solution. *Biochemistry* **45**, 2283–2293.

[117] Olsson B, Lautner R, Andreasson U, Öhrfelt A, Portelius E, Bjerke M, Hölttä M, Rosén C, Olsson C, Strobel G, Wu E, Dakin K, Petzold M, Blennow K, Zetterberg H (2016) CSF and blood biomarkers for the diagnosis of Alzheimer's disease: a systematic review and meta-

analysis. *Lancet Neurol* **15**, 673–684.
[118] Klunk WE, Engler H, Nordberg A, Wang Y, Blomqvist G, Holt DP, Bergström M, Savitcheva I, Huang G-F, Estrada S, Ausén B, Debnath ML, Barletta J, Price JC, Sandell J, Lopresti BJ, Wall A, Koivisto P, Antoni G, Mathis CA, Långström B (2004) Imaging brain amyloid in Alzheimer's disease with Pittsburgh Compound-B. *Ann. Neurol.* **55**.
[119] Chhatwal JP, Schultz AP, Marshall GA, Boot B, Gomez-Isla T, Dumurgier J, LaPoint M, Scherzer C, Roe AD, Hyman BT, Sperling RA, Johnson KA (2016) Temporal T807 binding correlates with CSF tau and phospho-tau in normal elderly. *Neurology* **87**, 920–926.
[120] Schöll M, Maass A, Mattsson N, Ashton NJ, Blennow K, Zetterberg H, Jagust W (2018) Biomarkers for tau pathology. *Mol. Cell. Neurosci.*
[121] Mattsson N, Zetterberg H, Janelidze S, Insel PS, Andreasson U, Stomrud E, Palmqvist S, Baker D, Tan Hehir CA, Jeromin A, Hanlon D, Song L, Shaw LM, Trojanowski JQ, Weiner MW, Hansson O, Blennow K, ADNI Investigators (2016) Plasma tau in Alzheimer disease. *Neurology* **87**, 1827–1835.
[122] Ai H-W, Henderson JN, Remington SJ, Campbell RE (2006) Directed evolution of a monomeric, bright and photostable version of Clavularia cyan fluorescent protein: structural characterization and applications in fluorescence imaging. *Biochem. J.* **400**, 531–540.
[123] Day RN, Booker CF, Periasamy A (2008) Characterization of an improved donor fluorescent protein for Forster resonance energy transfer microscopy. *J Biomed Opt* **13**, 031203.
[124] Nagai T, Ibata K, Park ES, Kubota M, Mikoshiba K, Miyawaki A (2002) A variant of yellow fluorescent protein with fast and efficient maturation for cell-biological applications. *Nat. Biotechnol.* **20**, 87–90.
[125] Sun Y, Day RN, Periasamy A (2011) Investigating protein-protein interactions in living cells using fluorescence lifetime imaging microscopy. *Nature Protocols* **6**, 1324–1340.
[126] Sun Y, Periasamy A (2014) Localizing Protein–Protein Interactions in Living Cells Using Fluorescence Lifetime Imaging Microscopy. In *Advanced Fluorescence Microscopy* Springer New York, New York, NY, pp. 83–107.
[127] Porzig R, Singer D, Hoffmann R (2007) Epitope mapping of mAbs AT8 and Tau5 directed against hyperphosphorylated regions of the human tau protein. *Biochem. Biophys. Res. Commun.* **358**, 644–649.
[128] Sengupta U, Portelius E, Hansson O, Farmer K, Castillo-Carranza D, Woltjer R, Zetterberg H, Galasko D, Blennow K, Kayed R (2017) Tau oligomers in cerebrospinal fluid in Alzheimer's disease. *Ann Clin Transl Neurol* **4**, 226–235.
[129] Patterson KR, Remmers C, Fu Y, Brooker S, Kanaan NM, Vana L, Ward S, Reyes JF, Philibert K, Glucksman MJ, Binder LI (2011) Characterization of prefibrillar Tau oligomers in vitro and in Alzheimer disease. *Journal of Biological Chemistry* **286**, 23063–23076.
[130] Elangovan M, Wallrabe H, Chen Y, Day RN, Barroso M, Periasamy A

(2003) Characterization of one- and two-photon excitation fluorescence resonance energy transfer microscopy. *Methods* **29**, 58–73.

[131] Sun Y, Rombola C, Jyothikumar V, Periasamy A (2013) Förster resonance energy transfer microscopy and spectroscopy for localizing protein-protein interactions in living cells. *Cytometry A* **83**, 780–793.

[132] Wallrabe H, Svindrych Z, Alam SR, Siller KH, Wang T, Kashatus D, Hu S, Periasamy A (2018) Segmented cell analyses to measure redox states of autofluorescent NAD(P)H, FAD & Trp in cancer cells by FLIM. *Sci Rep* **8**, 79.

[133] Di Primio C, Quercioli V, Siano G, Rovere M, Kovacech B, Novak M, Cattaneo A (2017) The Distance between N and C Termini of Tau and of FTDP-17 Mutants Is Modulated by Microtubule Interactions in Living Cells. *Front Mol Neurosci* **10**, 210.

[134] Bloom GS (2014) Amyloid-β and tau: the trigger and bullet in Alzheimer disease pathogenesis. *JAMA Neurol* **71**, 505–508.

[135] Kar S, Fan J, Smith MJ, Goedert M, Amos LA (2003) Repeat motifs of tau bind to the insides of microtubules in the absence of taxol. *EMBO J.* **22**, 70–77.

[136] Hamidi N, Nozad A, Sheikhkanloui Milan H, Amani M (2019) Okadaic acid attenuates short-term and long-term synaptic plasticity of hippocampal dentate gyrus neurons in rats. *Neurobiol Learn Mem* **158**, 24–31.

[137] Tepper K, Biernat J, Kumar S, Wegmann S, Timm T, Hübschmann S, Redecke L, Mandelkow E-M, Müller DJ, Mandelkow E (2014) Oligomer formation of tau protein hyperphosphorylated in cells. *Journal of Biological Chemistry* **289**, 34389–34407.

[138] Kaniyappan S, Chandupatla RR, Mandelkow E-M, Mandelkow E (2017) Extracellular low-n oligomers of tau cause selective synaptotoxicity without affecting cell viability. *Alzheimers Dement* **13**, 1270–1291.

[139] Arendt T, Brückner MK, Mosch B, Lösche A (2010) Selective cell death of hyperploid neurons in Alzheimer's disease. *Am. J. Pathol.* **177**, 15–20.

[140] Yang T, Li S, Xu H, Walsh DM, Selkoe DJ (2017) Large Soluble Oligomers of Amyloid β-Protein from Alzheimer Brain Are Far Less Neuroactive Than the Smaller Oligomers to Which They Dissociate. *Journal of Neuroscience* **37**, 152–163.

[141] Lei M, Xu H, Li Z, Wang Z, O'Malley TT, Zhang D, Walsh DM, Xu P, Selkoe DJ, Li S (2016) Soluble Aβ oligomers impair hippocampal LTP by disrupting glutamatergic/GABAergic balance. *Neurobiol. Dis.* **85**, 111–121.

[142] Varvel NH, Bhaskar K, Patil AR, Pimplikar SW, Herrup K, Lamb BT (2008) Abeta oligomers induce neuronal cell cycle events in Alzheimer's disease. *J. Neurosci.* **28**.

[143] Norambuena A, Wallrabe H, Cao R, Wang DB, Silva A, Svindrych Z,

Periasamy A, Hu S, Tanzi RE, Kim DY, Bloom GS (2018) A novel lysosome-to-mitochondria signaling pathway disrupted by amyloid-β oligomers. *EMBO J.* **37**, e100241.

[144] Zempel H, Thies E, Mandelkow E, Mandelkow E-M (2010) Abeta oligomers cause localized Ca(2+) elevation, missorting of endogenous Tau into dendrites, Tau phosphorylation, and destruction of microtubules and spines. *Journal of Neuroscience* **30**, 11938–11950.

[145] Norambuena A, Wallrabe H, McMahon L, Silva A, Swanson E, Khan SS, Baerthlein D, Kodis E, Oddo S, Mandell JW, Bloom GS (2017) mTOR and neuronal cell cycle reentry: How impaired brain insulin signaling promotes Alzheimer's disease. *Alzheimers Dement* **13**, 152–167.

[146] Parness J, Horwitz SB (1981) Taxol binds to polymerized tubulin in vitro. *J. Cell Biol.* **91**, 479–487.

[147] Yang C-PH, Horwitz SB (2017) Taxol®: The First Microtubule Stabilizing Agent. *Int J Mol Sci* **18**, 1733.

[148] Samsonov A, Yu J-Z, Rasenick M, Popov SV (2004) Tau interaction with microtubules in vivo. *J. Cell. Sci.* **117**, 6129–6141.

[149] Chun W, Waldo GS, Johnson GVW (2007) Split GFP complementation assay: a novel approach to quantitatively measure aggregation of tau in situ: effects of GSK3beta activation and caspase 3 cleavage. *Journal of Neurochemistry* **103**, 2529–2539.

[150] Kodama Y, Hu C-D (2012) Bimolecular fluorescence complementation (BiFC): A 5-year update and future perspectives. *Biotech* **53**.

[151] Anderie I, Schmid A (2007) In vivo visualization of actin dynamics and actin interactions by BiFC. *Cell Biol. Int.* **31**, 1131–1135.

[152] Guo Y, Rebecchi M, Scarlata S (2005) Phospholipase Cbeta2 binds to and inhibits phospholipase Cdelta1. *Journal of Biological Chemistry* **280**, 1438–1447.

[153] Duff K, Kuret J, Congdon EE (2010) Disaggregation of tau as a therapeutic approach to tauopathies. *Curr Alzheimer Res* **7**, 235–240.

[154] Lasagna-Reeves CA, Castillo-Carranza DL, Sengupta U, Sarmiento J, Troncoso J, Jackson GR, Kayed R (2012) Identification of oligomers at early stages of tau aggregation in Alzheimer's disease. *The FASEB journal : official publication of the Federation of American Societies for Experimental Biology*.

[155] Castillo-Carranza DL, Sengupta U, Guerrero-Muñoz MJ, Lasagna-Reeves CA, Gerson JE, Singh G, Estes DM, Barrett ADT, Dineley KT, Jackson GR, Kayed R (2014) Passive immunization with Tau oligomer monoclonal antibody reverses tauopathy phenotypes without affecting hyperphosphorylated neurofibrillary tangles. *Journal of Neuroscience* **34**, 4260–4272.

[156] Park J-C, Han S-H, Yi D, Byun MS, Lee JH, Jang S, Ko K, Jeon SY, Lee Y-S, Kim YK, Lee DY, Mook-Jung I, KBASE Research Group

(2019) Plasma tau/amyloid-β1–42 ratio predicts brain tau deposition and neurodegeneration in Alzheimer's disease. *Brain* **7**, 270.

[157] Iqbal K, Gong C-X, Liu F (2013) Hyperphosphorylation-induced tau oligomers. *Front Neurol* **4**, 112.

[158] Alonso A, Zaidi T, Novak M, Grundke-Iqbal I, Iqbal K (2001) Hyperphosphorylation induces self-assembly of tau into tangles of paired helical filaments/straight filaments. *Proc. Natl. Acad. Sci. U.S.A.* **98**, 6923–6928.

1